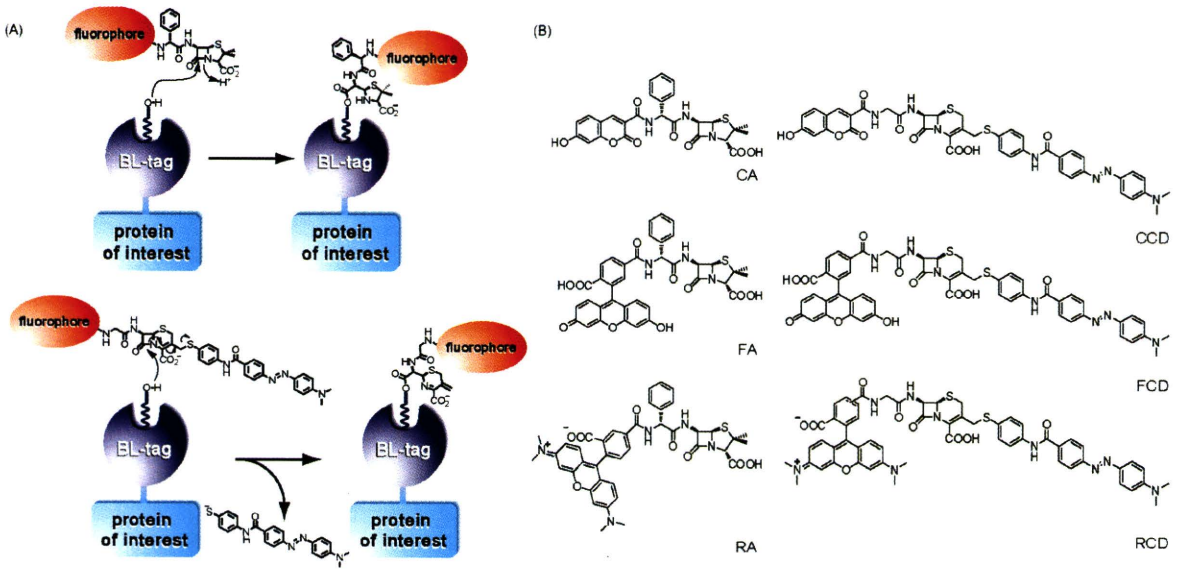

Figure 1. (A) General labeling mechanisms of the ampicillin- and cephalosporin-based probes. (B) Structures of β-lactam derivatives used for fluorescence labeling of BL-tag fusion proteins.

glycerol, and 10% mercaptoethanol) and resolved by NuPAGE (12% bis-Tris gel, Invitrogen). The fluorescence images of the gels were captured using a digital camera (Nikon COOLPIX P6000). The gels were stained with Coomassie Brilliant Blue prior to the capture of images.

Labeling of Cell Surface pcDNA3.1(+)-^{E166N}TEM-EGFR (BL-EGFR) with Various Probes. HEK293T cells maintained in 10% FBS in DMEM (Invitrogen) at 37 °C under 5% CO_2 were transfected with a plasmid coding for BL-EGFR, which was prepared as described previously (*16*), using Lipofectamine 2000 (Invitrogen). After 5−6 h, the culture medium was replaced with DMEM (without phenol red), and the cells were incubated at 37 °C for 24 h. The cells were then washed three times with DMEM (without phenol red) and incubated with 10 μM labeling probes in a CO_2 incubator for 30 min for CA, FA, and RA, or for 2 h for CCD and FCD. The cell nuclei were co-stained with Hoechst 33342 (100 ng mL^{-1}). After washing with DMEM containing 10% FBS, cells were incubated with HBSS, and the fluorescence images were captured with appropriate filter sets for each of the fluorophores.

Analysis of Fluorescence Images. Labeled cell images with CA, CCD, FA, and RA were acquired according to the above-mentioned procedure. 256 × 256 pixels area, where cells were confluently cultured, was selected at random from the acquired fluorescence images. The average fluorescence intensity of different colors per pixel was computed from the selected area using *MetaMorph* imaging software.

Multilabeling of Cells with BL-tag and SNAP-tag. Plasmids coding for BL-EGFR and COX8-2-SNAP were co-transfected into HEK293T cells. The cells were then incubated with FA, SNAP-Cell TMR Star, and Hoechst 33342 in a CO_2 incubator for 30 min (final concn of FA, 10 μM; SNAP-Cell TMR Star, 0.8 μM; Hoechst 33342, 100 ng mL^{-1}), and the fluorescence images were captured. The detailed procedure was the same as the procedure followed for the single protein labeling.

Western Blot Analysis of EGFR and BL-EGFR Expressed in HEK293T Cells after EGF Stimulation. HEK293T cells were transfected with BL-EGFR or pcDNA3.1(+)-EGFR using Lipofectamine 2000. After 5−6 h, the culture medium was replaced with DMEM, and the cells were incubated at 37 °C for 24 h. Prior to EGF addition, the cells were incubated overnight in the medium containing 0.5% serum. The cells were then washed once with PBS (−) and treated with EGF (100 ng mL^{-1}, Sigma, E9644) for 10 min at 25 °C. After one rinse with PBS (−), the cells were lysed with 200 μL of 1× SDS gel loading buffer (50 mM Tris−HCl buffer (pH 6.8), 1.3% SDS, 10% glycerol, and 5% mercaptoethanol). After scraping, the lysates were boiled at 95 °C for 3 min. Subsequently, samples were electrophoresed in a 7.5% or 10% SDS-polyacrylamide gel and transferred to PVDF membranes for Western blot. Membranes were blocked by 1 h incubation with TBST buffer (0.01% Tween 20, 138 mM NaCl, 20 mM Tris, pH 7.6) containing 5% skim milk (for anti-EGFR, anti-β-lactamase, and anti-β-actin antibodies) or 3% BSA (for anti-EGFR-pY1197 antibody) at room temperature. Then, anti-EGFR (1:500 dilution), anti-β-lactamase (1:5000 dilution), anti-EGFR-pY1197 (1:500 dilution), or anti-β-actin (1:5000 dilution) antibodies were added to each membrane. After incubation for 16 h at 4 °C with shaking, the membranes were washed three times with TBST buffer, incubated with horseradish peroxidase-linked secondary antibody, washed with TBST buffer, and visualized using ECL Western blotting detection reagents.

Immunofluorescence Detection of the Tyrosine Phosphorylation on BL-EGFR after EGF Stimulation. Transfected HEK293T cells were prepared and treated with EGF according to the above-mentioned procedure. After one rinse with PBS(−), the cells were fixed with 3.7% formaldehyde/PBS(−) at 25 °C for 20 min. After two rinses with PBS(−), the cells were blocked with blocking buffer (PBS containing 5% Goat Serum (Invitrogen) and 0.05% NaN_3) at 25 °C for 1 h. Anti-EGFR-pY1197 antibody, followed by fluorescein-conjugated goat antimouse antibody, was used to stain BL-EGFR or EGFR. After mounting, microscopic images were acquired using a filter set for fluorescein.

RESULTS AND DISCUSSION

Design and Synthesis of Fluorophores for the Labeling of BL-tag Fusion Proteins. Although it was previously shown that BL-tag fusion proteins can be specifically labeled with 7-hydroxycoumarin-conjugated β-lactam probes (Figure 1), the fluorescence was found to be dim and the excitation wavelength was short and hindered by the intrinsic autofluorescence of mammalian cells. The use of brighter and longer-excitation wavelength fluorophores is advantageous for various functional

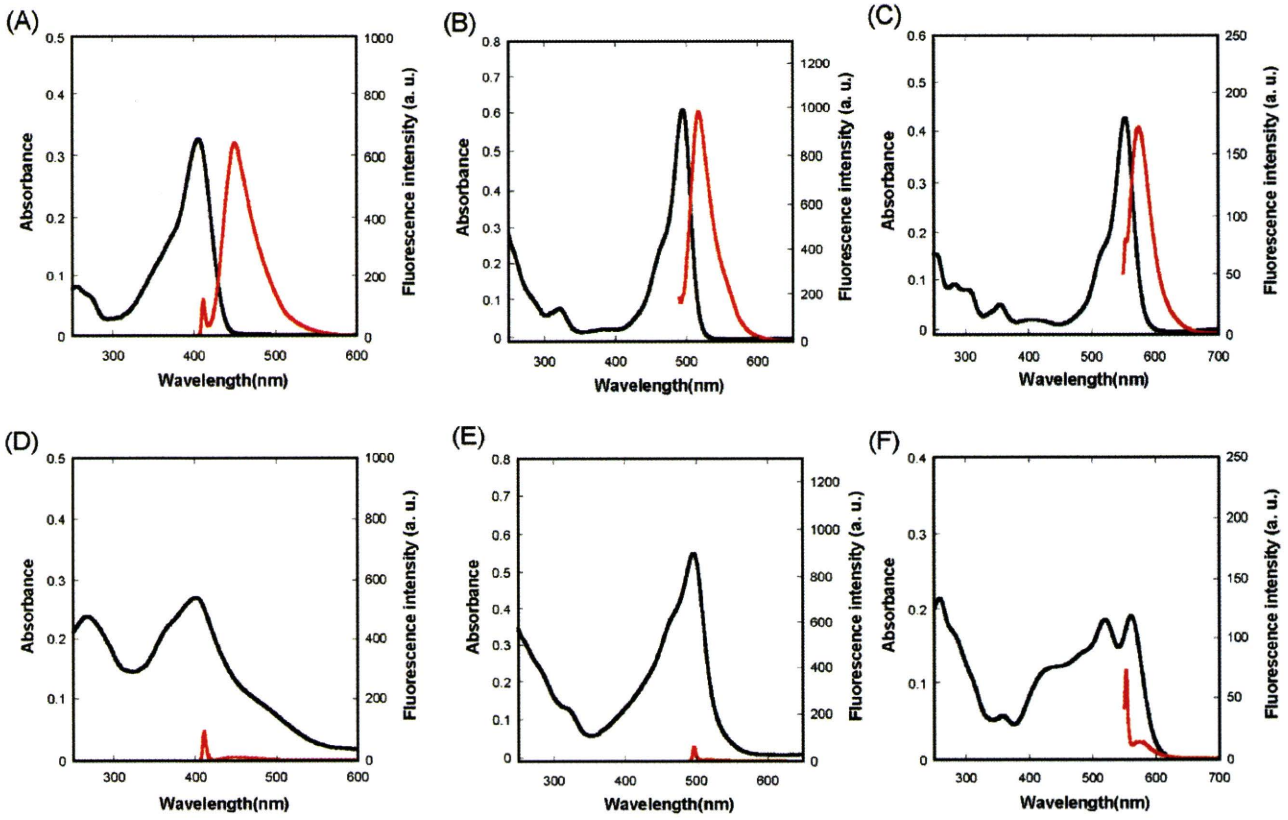

Figure 2. Absorption (black line) and emission spectra (red line) of (A) CA, (B) FA, (C) RA, (D) CCD, (E) FCD, and (F) RCD in 100 mM HEPES buffer (pH 7.4). In the absorption measurements, the probe concentrations were 5 μM for FA, FCD, RA, and RCD and 10 μM for CA and CCD. In the absorption measurements, the probe concentrations were 0.5 μM for FA, FCD, RA, and RCD and 1 μM for CA and CCD. Excitation wavelengths were 405 nm for CA and CCD, 492 nm for FA, 496 nm for FCD, and 553 nm for RA and RCD.

Table 1. Spectroscopic Properties and Calculated Values for FRET of Labeling Probes in 100 mM HEPES Buffer (pH 7.4)

compound	$\lambda_{abs,\ max}$/nm	$\lambda_{em,\ max}$/nm	fluorescence quantum efficiency (Φ)	Förester distance[a] (R_0)/Å	donor−acceptor distance[b] (R)/Å	energy transfer efficiency[c] (E)
CA	405	453	0.40	–	–	–
CCD	400	450	0.006	44.2	26.3	0.96
FA	492	517	0.71	–	–	–
FCD	496	520	0.005	43.4	27.8	0.93
RA	553	575	0.49	–	–	–
RCD	525, 565	573	0.07	19.6	27.7	0.12

[a] R_0 values were derived from the overlap integral between the absorption spectrum of DABCYL and the fluorescence spectrum of CA for CCD, FA for FCD, and RA for RCD. [b] R values were evaluated from the farthest distance between the fluorophore and DABCYL by using the molecular modeling software. [c] Energy transfer efficiencies were calculated from the equation $E = R_0^6/(R_0^6 + R^6)$.

studies using living cells. Therefore, β-lactam probes conjugated to fluorescein or tetramethylrhodamine (TAMRA) were designed and synthesized (Figure 1B). The fluorescence labeling probes FA and RA were synthesized in one step from ampicillin and activated esters of the corresponding fluorophores. FCD and RCD, which were designed to be fluorogenic as well as CCD, were also synthesized. RCD was synthesized from the activated ester of the 5(6)-TAMRA isomers and used for the experiments without separation of the 5(6)-isomers (see Figure S1 in Supporting Information).

Absorption and emission spectra of all β-lactam labeling probes are shown in Figure 2, and the spectroscopic properties are summarized in Table 1. FA and RA exhibited similar spectroscopic properties to fluorescein and TAMRA, respectively. From the Förster radii caluculated from their spectra and the simulated donor−acceptor distances, the FRET efficiency was estimated (Table 1). We predicted that FCD fluorescence would be quenched sufficiently from the FRET efficiency value. Indeed, FCD was largely quenched by intramolecular FRET from coumarin to DABCYL (Φ = 0.005). In contrast, RCD fluorescence would theoretically not be quenched because of the limited overlap between the absorption spectrum of DABCYL and the emission spectrum of TAMRA. Nevertheless, RCD fluorescence was considerably quenched (Φ = 0.07). This quenching of RCD fluorescence can be ascribed to the intramolecular association between TAMRA and DABCYL moieties. We previously reported that, if two hydrophobic dyes are located in close proximity, self-quenching occurs due to the close contact of the two dyes in aqueous solution (*29*). The fluorescence intensities of FCD and RCD were recovered by the addition of WT TEM-1 and BL-tag in a time-dependent manner (see Figure S2 in Supporting Information). These results indicate that elimination of the DABCYL moieties occurs by the enzymatic cleavage of the β-lactam in both cases. The labeling capabilities of all compounds with BL-tag were confirmed by SDS-PAGE (see Figure S3 in Supporting Information).

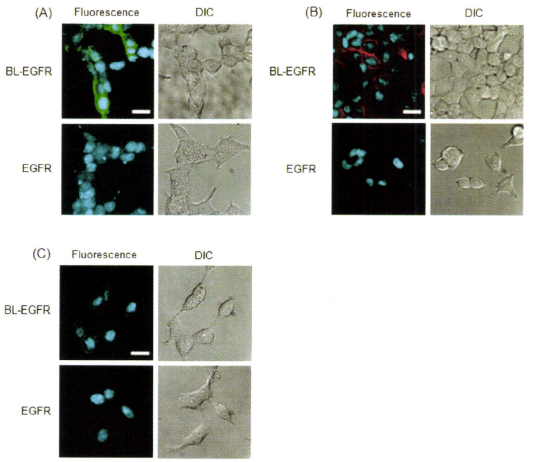

Figure 3. Labeling of BL-tag fusion proteins with (A) FA, (B) RA, and (C) FCD. HEK293T cells were transfected with a plasmid encoding BL-EGFR or EGFR. The cell nuclei were costained with Hoechst 33342. For fluorescence microscopic images, the cells were excited at 330−385 nm for Hoechst 33342, 460−490 nm for FA, and 510−550 nm for RA. Scale bar: 20 μm.

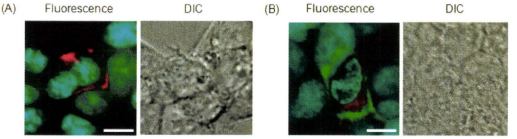

Figure 4. (A) Multicolor imaging of HEK293T cells expressing BL-EGFR. BL-EGFR, nuclei, and cytosol were labeled with RA (red), Hoechst 33342 (cyan), and CellTracker Green (green), respectively. (B) Multiprobe labeling of HEK293T cells expressing BL-EGFR and COX8-2-SNAP. BL-EGFR was labeled with FA, COX-8-2-SNAP with SNAP-Cell TMR-STAR, and nuclei with Hoechst 33342. Fluorescence microscopic images were excited at 330−385 nm, 460−490 nm, and 510−550 nm. Scale bar: 10 μm.

Fluorescence Labeling of BL-tag Fusion Proteins by the Synthesized Probes. BL-tag was fused to the N-terminus of epidermal growth factor receptor (EGFR), and the fusion protein BL-EGFR was expressed on cell surfaces of HEK293T cells by transfection with a plasmid encoding BL-EGFR. The cells were incubated with FA or RA, washed three times, and observed using a fluorescence microscope. The cells generating BL-EGFR clearly emitted green or red fluorescence at the plasma membrane (Figure 3A,B). We calculated the average fluorescence intensity per pixel from BL-EGFR expressing cells and negative control cells, and compared with each other (see Figure S4 in Supporting Information). As a result, the fluorescence signal from labeled cells by FA or RA was clearly enhanced compared with the background signal (about 1.8 times), while the fluorescence signal of cells labeled by CA or CCD was about 10% higher than the background signal. Therefore, the signal-to-background ratio was largely improved by FA and RA relative to CA and CCD. Subsequently, the labeling properties of FCD were investigated. The cells generating BL-EGFR were labeled by FCD in a labeling procedure similar to the procedure used for FA and RA (Figure 3C).

Multicolor Imaging by Simultaneous Labeling with BL-tag and SNAP-tag. We applied BL-tag technology to multicolor imaging of cells in order to demonstrate its wide versatility. After transfection of HEK293T cells with a plasmid encoding BL-EGFR, Hoechst 33342, CellTracker Green, and RA were incubated. Cells were then imaged using different fluorophores with appropriate filter sets. Each organelle was confirmed by multicolor fluorescence imaging (Figure 4A). In addition, BL-tag fusion proteins were found to be labeled with different color fluorophores (Figure 3). This property is beneficial for pulse-chase fluorescence imaging experiments used for tracing protein trafficking after various stimulations (*30, 31*).

Next, multicolor fluorescence labeling of two different target proteins was performed with another specific protein labeling system known as SNAP-tag technology. In this experiment, SNAP-tag was applied as a COX8-2-SNAP fusion plasmid encoding COX8-2 (subunit 8-2 protein of cytochrome c oxidase) cloned upstream of SNAP-tag. Cytochrome c oxidase is a terminal enzyme of the respiratory transport chain and localized at the inner mitochondrial membrane (*32*). The COX8-2-SNAP fusion proteins provide fluorescence in mitochondria when labeled with SNAP-Cell TMR-Star.

HEK293T cells were co-transfected with BL-EGFR and COX8-2-SNAP plasmids. The cells were incubated with FA, SNAP-Cell TMR-Star, and Hoechst 33342, and then washed three times with DMEM containing 10% FBS prior to imaging with a fluorescence microscope. Though the co-expression

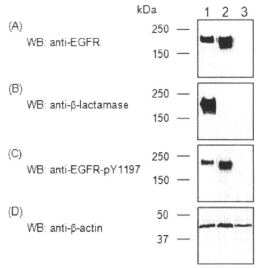

Figure 5. Western blot analysis of the EGFR and BL- EGFR expressed in transfected HEK293T cells after EGF stimulation. (A) Detection of EGFR with polyclonal anti-EGFR antibody. (B) Detection of TEM-1 with polyclonal anti-β-lactamase antibody. (C) Detection of phosphorylated tyrosine at 1197 position with monoclonal anti-EGFR-pY1197 antibody. (D) Detection of β-actin cytoskeleton with monoclonal anti-β-actin antibody. Lane 1: BL-EGFR-expressing cells. Lane 2: EGFR-expressing cells. Lane 3: Cells transfected with an empty plasmid vector.

efficiencies were not very good in this experiment, green fluorescence derived from FA was observed along the plasma membrane and red fluorescence from SNAP-Cell substrates in mitochondria was observed in the same cells (Figure 4B). This result distinctly indicates that BL-tag and SNAP-tag have nonoverlapping substrate specificity and can be used simultaneously in single cells.

Ligand-Induced Activation of the BL-tag Fusion Protein. Finally, we demonstrate the low interference of BL-tag with the function of the target protein EGFR. EGFR is a 170 kDa transmembrane glycoprotein that belongs to a tyrosine kinase receptor family comprising four members. The intracellular trafficking behavior and ligand-dependent dimerization of EGFR has attracted great attention (*33*). It was, however, reported that the expression and trafficking of EGFR was greatly disrupted as a result of extracellular GFP fusion and appropriate expression of the fusion protein was not detected by Western blot analysis with anti-GFP antibody (*34*) due to the fact that the fluorophore formation of GFP strongly depends upon the structural integrity of the protein (*3*). The identity of the BL-EGFR fusion protein was characterized by Western blot analysis with anti-β-lactamase, anti-EGFR, and anti-EGFR-pY1197 phosphorylation site-specific antibodies. Specific ligand binding on the extracellular domain of EGFR results in dimerization of the receptor and subsequent autophosphorylation of the tyrosine residues, the most predominant of which is pY1197 (*35*).

HEK293T cells were transfected with fusion proteins or EGFR plasmids, followed by incubation under serum-starved conditions. The cells were then stimulated with EGF and analyzed by Western blot. Naive (nontransfected) HEK293T cells express extremely low levels of endogenous EGFR as demonstrated in cells transfected with a control plasmid vector probed with an anti-EGFR antibody (lane 3 in Figure 5A) (*36*). When lysates of the cells transfected with EGFR plasmids were probed with an anti-EGFR antibody, one major band was visible with a molecular weight of about 170 kDa, corresponding to EGFR (lane 2 in Figure 5A). A single band was also detected from cells transfected with BL-EGFR. This band appeared in the slightly upper position of that of EGFR. This is consistent with the increase of the molecular weight as a result of fusion of BL-tag to EGFR (lane 1 in Figure 5A). On the other hand, when the membrane was probed with an anti-β-lactamase antibody, the immunoblotted band was observed only in the lane of the lysate containing BL-EGFR fusion protein (Figure 5B). These results suggest that the BL-EGFR fusion protein was properly expressed in HEK293T cells.

After stimulation by EGF, phosphorylation of Y1197 was confirmed using an anti-EGFR-pY1197 antibody. A single band shows that phosphorylation was observed in the lanes of cell lysates containing BL-EGFR or EGFR (lanes 1 and 2 in Figure 5C). In addition, we compared the distribution of BL-EGFR and EGFR after EGF stimulation by immunofluorescence staining with anti-EGFR-pY1197 antibody. Cells expressing BL-EGFR and EGFR gave the same distribution pattern of fluorescence responses that demonstrate phosphorylation in the cells (see Figure S5 in Supporting Information). From these results, it is evident that the phosphorylation function of EGFR can be preserved after introduction of the BL-tag to the extracellular domain of EGFR. All of the results discussed herein suggest that BL-tag has lower interference than GFP with respect to the function of EGFR.

In conclusion, we have designed and synthesized various labeling probes for BL-tag. These new probes have superior spectroscopic properties relative to the previously reported probes, CA and CCD. FA and RA can specifically label BL-tag in living cells, while FCD and RCD possess fluorogenic properties based on FRET or intramolecular stacking interaction which provides a useful switching mechanism for protein labeling probes, as we recently reported (*37*). The function of EGFR was found to be considerably preserved after the fusion of BL-tag to the extracellular domain. This low interference with the function of the target protein can provide a great advantage relative to fusion to GFP and should be suitable for studying the function or trafficking of POIs. Furthermore, BL-tag technology can be simultaneously used with other protein labeling methods such as SNAP-tag technology. Orthogonality of the substrate specificity between BL-tag and SNAP-tag was also shown.

In the future, a series of labeling probes with various fluorophores for BL-tag can be applied to a pulse-chase experiment that can distinguish between young and old copies of proteins by labeling at different time points with different fluorophores. Moreover, protein labeling techniques can be used not only for fluorescence imaging, but also for inducers of protein−protein interactions. Techniques based on multiple protein labeling methods are quite useful for studying and controlling protein−protein interactions (*38, 39*). Thus, we have provided a potential tool for practical biological applications. BL-tag technology can be exploited with conventional protein labeling methods for the specific labeling of two or more different proteins within a single cell. Furthermore, combinations of BL-tag technology with other imaging methods such as MRI or NIR are expected to contribute to the clarification of various protein−protein interactions.

ACKNOWLEDGMENT

This work was supported in part by the Grant-in-Aid for Scientific Research from the Ministry of Education, Culture, Sports, Science and Technology (MEXT) of Japan, by the Grant-in-Aid from the Ministry of Health, Labour and Welfare (MHLW) of Japan, and by the New Energy and Industrial Technology Development Organization (NEDO) of Japan. K.K. expresses his special thanks for support from the Takeda Science Foundation. S.W. acknowledges support from a Global COE Fellowship of Osaka University and a JSPS Research Fellowship.

Supporting Information Available: Materials and Instruments; synthetic details and characterization of FA, FCD, RA and RCD; supplementary figures. This material is available free of charge via the Internet at http://pubs.acs.org.

LITERATURE CITED

(1) Giepmans, B. N. G., Adams, S. R., Ellisman, M. H., and Tsien, R. Y. (2006) The fluorescent toolbox for assessing protein location and function. *Science 312*, 217–224.

(2) Phillips, G. N., Jr. (1997) Structure and dynamics of green fluorescent protein. *Curr. Opin. Struct. Biol. 7*, 821–827.

(3) Lisenbee, C. S., Karnic, S. K., and Trelease, R. T. (2003) Overexpression and mislocalization of a tail-anchored GFP redefines the identity of peroxisomal ER. *Traffic 4*, 491–501.

(4) Griffin, B. A., Adams, S. R., and Tsien, R. Y. (1998) Specific covalent labeling of recombinant protein molecules inside live cells. *Science 281*, 269–272.

(5) Griffin, B. A., Adams, S. R., Jones, J., and Tsien, R. Y. (2000) Fluorescent labeling of recombinant proteins in living cells with FLAsH. *Methods Enzymol. 327*, 565–578.

(6) Adams, S. R., Campbell, R. E., Gross, L. A., Martin, B. R., Walkup, G. K., Yao, Y., Llopis, J., and Tsien, R. Y. (2002) New biarsenical ligands and tetracystein motif for protein labeling *in vitro* and *in vivo*. Synthesis and biological applications. *J. Am. Chem. Soc. 124*, 6063–6076.

(7) Los, G. V., et al. (2008) Halotag: A novel protein labeling technology for cell imaging and protein analysis. *ACS Chem. Biol. 3*, 373–382.

(8) Keppler, A., Gendreizig, S., Pick, H., Vogel, H., and Johnsson, K. (2003) A general method for the covalent labeling of fusion proteins with small molecules *in vivo*. *Nat. Biotechnol. 21*, 86–89.

(9) Kindermann, M., Sielaff, I., and Johnsson, K. (2004) Synthesis and characterization of bifunctional probes for the specific labeling of fusion proteins. *Bioorg. Med. Chem. Lett. 14*, 2725–2728.

(10) Keppler, A., Pick, H., Arrivoli, C., Vogel, H., and Johnsson, K. (2004) Labeling of fusion proteins with synthetic fluorophores in live cells. *Proc. Natl. Acad. Sci. U.S.A. 101*, 9955–9959.

(11) Miller, L. W., Sable, J., Goelet, P., Sheetz, M. P., and Cornish, V. W. (2004) Methotrexate conjugates: A molecular *in vivo* protein tag. *Angew. Chem., Int. Ed. 43*, 1672–1675.

(12) Chen, I., Howarth, M., Lin, W., and Ting, A. Y. (2005) Site-specific labeling of cell surface proteins with biophysical probes using biotin ligase. *Nat. Methods 2*, 99–104.

(13) Lin, C.-W., and Ting, A. Y. (2006) Transglutaminase-catalyzed site-specific conjugation of small molecule probes to proteins *in vitro* and on the surface of living cells. *J. Am. Chem. Soc. 128*, 4542–4543.

(14) Hauser, C. T., and Tsien, R. Y. (2007) A hexahistidine-Zn^{2+}-dye label reveals STIM1 surface exposure. *Proc. Natl. Acad. Sci. U.S.A. 104*, 3693–3697.

(15) Ojida, A., Honda, K., Shinmi, D., Kiyonaka, S., Mori, Y., and Hamachi, I. (2006) Oligo-Asp tag/Zn(II) complex probe as a new pair for labeling and fluorescence imaging of proteins. *J. Am. Chem. Soc. 128*, 10452–10459.

(16) Mizukami, S., Watanabe, S., Hori, Y., and Kikuchi, K. (2009) Covalent protein labeling based on non-catalytic β-lactamase and a designed FRET substrate. *J. Am. Chem. Soc. 131*, 5016–5017.

(17) Christensen, H., Martin, T. M., and Waley, S. G. (1990) β-lactamase as fully efficient enzymes. *Biochem. J. 266*, 853–861.

(18) Moore, J. T., Davis, S. T., and Dev, K. I. (1997) The development of β-lactamase as a highly versatile genetic reporter for eukaryotic cells. *Anal. Biochem. 247*, 203–209.

(19) Zlokarnik, G., Negulescu, P. A., Knapp, T. E., Mere, L., Burres, N., Feng, L., Whitney, M., Roemer, K., and Tsien, R. Y. (1998) Quantitation of transcription and clonal selection of single living cells with β-lactamase as reporter. *Science 279*, 84–88.

(20) Gao, W., Xing, B., Tsien, R. Y., and Rao, J. (2003) Novel fluorogenic substrates for imaging β-lactamase gene expression. *J. Am. Chem. Soc. 125*, 11146–11147.

(21) Fisher, F. J., Meroueh, S. O., and Mobashery, S. (2005) Bacterial resistance to β-lactam antibiotics: Compelling opportunism, compelling opportunity. *Chem. Rev. 105*, 395–424.

(22) Matagne, A., Lamotte-Blasseur, J., and Frére, J.-M. (1998) Catalytic properties of class A β-lactamases: efficiency and diversity. *Biochem. J. 330*, 581–598.

(23) Guillaume, G., Vanhove, M., Lamotte-Brasseur, J., Ledent, P., Jamin, M., Joris, B., and Frére, J.-M. (1997) Site-directed mutagenesis of glutamate 166 in two β-lactamases. *J. Biol. Chem. 272*, 5438–5444.

(24) Adachi, H., Ohta, T., and Matsuzawa, H. (1991) Site-directed mutants, at position 166, of RTEM-1 β-lactamase that form a stable acyl-enzyme intermediate with penicillin. *J. Biol. Chem. 266*, 3186–3191.

(25) Page, M. I., and Proctor, P. (1984) Mechanism of β-lactam ring opening in cephalosporins. *J. Am. Chem. Soc. 106*, 3820–3825.

(26) Nishikawa, Y., and Hiraki, K. (1984) Calculation of quantum efficiency of rhodamine derivatives. *Analytical Methods of Fluorescence and Phosphorescence*, p 76, Kyoritsu Publishing Company, Tokyo

(27) Parker, C. A., and Rees, W. T. (1960) Correction of fluorescence spectra and measurement of fluorescence quantum efficiency. *Analyst 85*, 587–600.

(28) Lakowicz, J. R. (2006) Calculation of Förster distance and Energy transfer efficiency. *Principle of Fluorescence Spectroscopy*, 3rd ed., pp 443−475, Chapter 13, Springer Science+Business Media, LLV, New York.

(29) Mizukami, S., Kikuchi, K., Higuchi, T., Urano, Y., Mashima, T., Tsuruo, T., and Nagano, T. (1999) Imaging of caspase-3 activation in HeLa cells stimulated with etoposide using a novel fluorescent probe. *FEBS Lett. 453*, 356–360.

(30) Gaietta, G., Deerinck, T. J., Adams, S. R., Bouwer, J., Tour, O., Laird, D. W., Sosinsky, G. E., Tsien, R. Y., and Ellisman, M. H. (2002) Multicolor and electron microscopic imaging of connexin trafficking. *Science 296*, 503–507.

(31) Vivero-Pol, L., George, N., Krumm, H., Johnsson, K., and Johnsson, N. (2005) Multicolor imaging of cell surface proteins. *J. Am. Chem. Soc. 127*, 12770–12771.

(32) Malmström, B. G. (1990) Cytochrome c oxidase as a redox-linked proton pump. *Chem. Rev. 90*, 1247–1260.

(33) Sorkin, A., and Goh, L. K. (2009) Endocytosis and intracellular trafficking of ErbBs. *Exp. Cell Res. 315*, 683–696.

(34) Brock, R., Hamelers, I. H. L., and Jovin, T. M. (1999) Comparison of fixation protocols for adherent cultured cells applied to a GFP fusion protein of the epidermal growth factor receptor. *Cytometry 35*, 353–362.

(35) Chattopadhyay, A., Vecchi, M., Ji, Q., Memaugh, R., and Carpenter, G. (1999) The role of individual SH2 domain in mediating association of phospholipase C-γ1 with the activated EGF receptor. *J. Biol. Chem. 274*, 26091–26097.

(36) Jones, S. M., Foreman, S. K., Shank, B. B., and Kurten, R. C. (2002) EGF receptor downregulation depends on a trafficking motif in the distal tyrosine kinase domain. *Am. J. Physiol. Cell Physiol. 282*, C420–C433.

(37) Hori, Y., Ueno, H., Mizukami, S., and Kikuchi, K. (2009) Photoactive yellow protein-based protein labeling system with turn-on fluorescence intensity. *J. Am. Chem. Soc. 131*, 16610–16611.

(38) Gendreizig, S., Kindermann, M., and Johnsson, K. (2003) Induced protein dimerization *in vivo* through covalent labeling. *J. Am. Chem. Soc. 125*, 14970–14971.

(39) Chidley, C., Mosiewicz, K., and Johnsson, K. (2008) A designed protein for the specific and covalent heteroconjugation of biomolecules. *Bioconjugate Chem. 19*, 1753–1756.

BC100333K

Turn-on fluorescence switch involving aggregation and elimination processes for β-lactamase-tag†

Kalyan K. Sadhu,[a] Shin Mizukami,[ab] Shuji Watanabe[a] and Kazuya Kikuchi*[ab]

Received 8th July 2010, Accepted 13th August 2010
DOI: 10.1039/c0cc02432e

The targeted protein of interest is fused with genetically modified β-lactamase enzyme, which reacts with the probe in physiological conditions to break the aggregated interaction between the fluorophore and quencher. This alliance–separation technique is new for protein labeling and is probed *in vitro* and in live cell imaging studies.

Molecular imaging with the aid of fluorescence microscopy has become an indispensable means to study the proceedings in living cells, which would be extensively valuable for the future of medical science. The practical approach involving chemistry to control modification and monitoring specific proteins has proved useful.[1] The direct imaging of protein interactions in single living cells is possible due to the site-specific labeling of proteins with molecular tags, which is an authoritative means for studying the structure–function relationships of proteins.[2] The rationale of fluorescence microscopy in cell biology has been thoroughly tailored with fluorescence proteins.[3] To conquer the shortcomings intrinsic to proteins due to the lack of robust modification for target phenomena and nonfluorogenicity, bright and photostable small fluorophores can be advantageous over their fluorescent protein counterparts.[4] Tetracysteine-tag and its modified version provided a route for using small molecules in fluorogenic labeling and were found to be effective for activation of G protein-coupled receptors in living cells.[5] Specificity towards labeling was observed with SNAP-tag and its modified version with semisynthetic fluorescent sensor proteins.[6] In our protein labeling method our aim was to combine fluorogenicity and specificity of the probe. Several other protein-[7] and enzyme-mediated[8] labeling methods have enriched the recent literature. Among the small fluorogenic molecules, fluorescein is approved by the U.S. Food and Drug Administration (FDA) for medical use.[9] Herein, we have chosen fluorescein for our protein labeling experiment.

Recently we have shown[10] a protein labeling system that coalesces genetically modified β-lactamase (BL-tag) with low molecular weight fluorogenic β-lactam probes. The study concerned FRET to optimize the emission of the probe. A shortcoming of the strategy involved the suitable choice of donor fluorophore, acceptor quencher and their application in physiological conditions. To surmount the restraint in the FRET process, our new approach is based on the switching mechanism involving aggregation followed by elimination processes. In the modified version, the quenching ability of the fluorescence quencher does not depend upon the emission wavelength of the fluorophore, as is desired for an effective FRET process. In this case the quenching phenomenon is the intrinsic property of the quencher part.

We have continued our study with the same BL-tag protein. The reaction of TEM-1 (class A β-lactamases) with β-lactam rings involves acylation and deacylation steps. Glu166 is indispensable for the deacylation step,[11] and the mutant version of TEM-1 (^{E166N}TEM or BL) restricts the deacylation step.[12] Our aim was to exploit the properties of BL for covalent attachment with a fluorescent substrate with a better versatile technique. Here, we present a rationally designed fluorogenic probe that takes advantage of the aggregation of fluorophore and quencher. In the aggregated form, the interaction between the fluorogenic part and the quencher restricts the emission of the fluorophore. The viability of the fluorescently labeled BL-tag under physiological situations has been explored with the newly designed and synthesized a cephalosporin-based fluorescent probe (**FCDNB**, Scheme 1a). We have used the *m*-dinitrobenzene (DNB) group as quencher, whose quenching efficiency is well established.[13] The probe contains 6-carboxyfluorescein as fluorophore and DNB as quencher and they are connected to different sides of the β-lactam ring of the central cephalosporin part. A flexible spacer can control the emission[14] and enzyme activity prompts

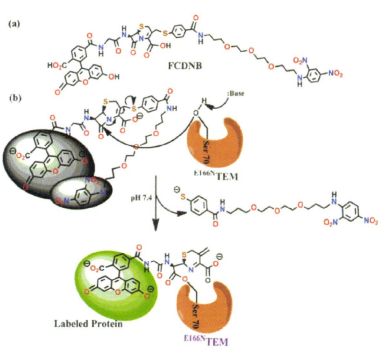

Scheme 1 Labeling strategy with (a) structure and (b) labeling state of the fluorescent probe **FCDNB**.

[a] *Division of Advanced Science and Biotechnology, Graduate School of Engineering, Osaka University, 2-1 Yamadaoka, Suita, Osaka 565-0871, Japan. E-mail: kkikuchi@mls.eng.osaka-u.ac.jp; Fax: (+81) 6-6879-7875*
[b] *Immunology Frontier Research Center, Osaka University, 2-1 Yamadaoka, Suita, Osaka 565-0871, Japan*

† Electronic supplementary information (ESI) available: Experimental details, chemical structures, UV-Visible absorption spectra, and fluorescence spectra of **FCDNB**. See DOI: 10.1039/c0cc02432e

the fluorescence recovery. This inspired us to introduce polyethylene glycol in the newly developed system for better aggregation interaction and solubility in physiological conditions. Incubation with BL-tag protein leads to the subsequent elimination of quencher to label the covalent modification of the tag protein with the desired fluorophore. Using this modification, we can achieve a new and better route to a turn-on fluorescence protein labeling system compared to our previous FRET analogue under the same physiological conditions. The advantage of this design principle is robustness towards fluorescein, whose fluorescence intensity was not easily modified by the previous design,[10] since the quenching mechanism is due to simple molecular interactions.

The labeling mechanism is illustrated in Scheme 1b. Cleavage of the β-lactam group of **FCDNB** by Ser70 in BL produced covalent labeling of the fluorescein to the protein with concomitant release of DNB. The labeled protein was detected by irradiating the gel with visible light (λ = 470 nm) in an SDS-PAGE study. A protein band of ~29 kDa was observed, exhibiting green fluorescence (Fig. 1a). To confirm that the labeling activity is due to the BL-tag, we carried out a similar experiment with wild-type (WT) TEM-1. In contrast to BL, incubation of WT TEM with **FCDNB** ended with no labeled fluorescence. Labeling in a biological medium with HEK293T cell lysate was also checked. SDS-PAGE analysis confirmed competent and selective labeling of **FCDNB** (Fig. 1b).

Compound **8** (Fig. S2†) with only DNB quencher showed maximum absorption at 364 nm and negligible absorption after 475 nm in HEPES buffer, whereas there is no substantial emission of fluorescein in this region (Fig. S3†). The probability of FRET from fluorescein to the DNB group can be overruled due to the insignificant overlap of fluorescein emission and DNB absorbance. The absorption peaks of fluorescein and the DNB group in **FCDNB** were obtained at 507 nm and 375 nm, respectively, in HEPES buffer. In methanol, the absorption peaks for both fluorescein and DNB were shifted by 10–15 nm (Fig. S4†). These positional shifts suggest a different nature of interaction between the fluorophore and quencher in the studied media.

The fluorescence quantum yield of **FCDNB** was found to be 0.05 in 100 mM HEPES buffer. This result confirmed that the fluorescein emission was sufficiently quenched because of intramolecular interaction between the fluorophore and DNB group. 2,4-Dinitroaniline is an efficient intramolecular fluorescence quencher for fluorescein labeled oligonucleotides.[15] The mechanism of fluorescence attenuation can be attributed to electron-rich aromatic rings that can π-stack with the electron-poor nitroaromatics.[16] The inherent quenching phenomenon of DNB does not depend upon the nature of fluorophores, rather it has been found effective in the case of several fluorogenic probes.[17] The quantum yield of **FCDNB** in methanol is 0.42. This significant difference of emissions in these two solutions (Fig. 2a) implies that the aggregation phenomenon is favorable in the physiological conditions only. Buffer comparison studies of **FCDNB** and the DNB-free version of the probe (**FA**, Fig. S5†) showed that **FCDNB** is sufficiently quenched in each buffer medium (Table S1†). A pH probe fluorescence assay of **FCDNB** (Fig. S6†) suggests that emission from fluorescein is more effective at physiological conditions compared to in acidic medium.

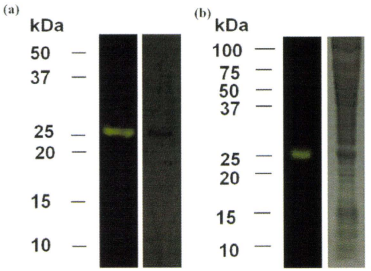

Fig. 1 **FCDNB** incubated fluorescence (left) and CBB-stained (right) gel images of (a) BL and (b) BL mixed with HEK293T cell lysate.

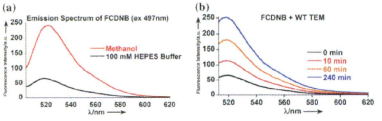

Fig. 2 (a) Emission spectra of **FCDNB** in 100 mM HEPES buffer (pH 7.4) and methanol (conc. of **FCDNB** 0.5 μM). (b) Time-dependent emission spectra (λ_{ex} = 507 nm) of **FCDNB** in the presence of WT TEM in 100 mM HEPES buffer (pH 7.4) containing 0.05% DMSO at 25 °C.

The effects of BL-tag and WT TEM on the emission properties of the probe were studied. The fluorescence intensity at 520 nm due to fluorescein was monitored after the incubation of BL with **FCDNB**. Slow enhancement of the fluorescence intensity was observed with time (Fig. S7†). This indicates that the cleavage of the β-lactam of **FCDNB** was performed by BL but the disaggregation followed by elimination of the DNB group is very slow. The process is significantly different in case of the incubation study with WT TEM. The DNB group was eliminated by WT TEM with a much faster rate and the fluorescence signal increased a considerable amount (Fig. 2b) as expected due to the favorable deacylation step of the catalytic activity. The change in fluorescence enhancement was found to be slow after 4 h. The initial rate of fluorescence enhancement in the case of WT TEM was found to be ~20 times that of the BL-tag. This noticeable difference in the rate of reaction is also due to the controlled acylation path as a result of mutation at Glu166.[10] In comparison, emission intensities of fluorescein in **FA** remain the same with time for both WT TEM and BL-tag.

The site-specific labeling of target proteins has been probed by the demonstration of **FCDNB** on the surface of living cells (Fig. 3a). For this purpose we have chosen the N-terminus of epidermal growth factor receptor (EGFR). The target fluorophore recognizes the transfected protein as a result of covalent bond formation. The BL-tag fused to the EGFR, and then it was expressed with HEK293T cells. After treatment with **FCDNB**, fluorescence images of the HEK293T cells were

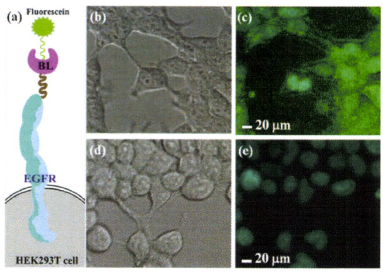

Fig. 3 (a) Labeling of protein with the probe through the BL-tag. (b)–(e) Optical microscopic images of **FCDNB**-labeled HEK293T cells expressing (b,c) BL-EGFR and (d,e) EGFR. (b,d) DIC images, (c,e) fluorescence microscopic images. The cell nuclei were stained with Hoechst 33342. For fluorescence microscope images, the cells were excited at 330–385 nm for Hoechst 33342, and 460–490 nm for **FCDNB**.

taken under an inverted fluorescence microscope. The cell nuclei were stained with Hoechst 33342. Only the cells expressing the BL-EGFR fusion protein emitted green fluorescence as a consequence of specific labeling by the probe (Fig. 3c). In the case of HEK293T cells expressing the EGFR protein without any BL-tag, the cell nuclei show only cyan fluorescence due to Hoechst 33342. In this case no fluorescein-labeled cell was observed (Fig. 3e).

In conclusion, we have modified our protein labeling method with an improved and straightforward technique that merges a BL-tag with a low molecular weight fluorogenic β-lactam probe. Through appropriate modification of our probe design, we succeeded in labeling targeted proteins with a familiar and useful fluorophore *in vitro* and also in living cells. Despite the similarity in molecular weight of the BL and Green Fluorescent Protein (GFP), fluorogenicity can be introduced through BL-tag technology, which is rather impossible with GFP. In this tailored version, the system can be considered as preliminary proof of a newly developed principle. By introducing a more efficiently quenched probe, this system can solve the problem of washing procedures after the labeling method. We are presently engaged in the aspect of the versatile use of this customized *modus operandi* with a range of fluorophores.

This research is supported by the Japan Society for the Promotion of Science (JSPS) through its "Funding Program for World-Leading Innovative R&D on Science and Technology (FIRST Program). This work was supported in part by the Grant-in-Aid for Scientific Research from the Ministry of Education, Culture, Sports, Science and Technology (MEXT) of Japan, the Grant-in-Aid from the Ministry of Health, Labour and Welfare (MHLW) of Japan, and the New Energy and Industrial Technology Development Organization (NEDO) of Japan. KK expresses his special thanks for support from the Takeda Science Foundation. KKS and SW acknowledge support from a Global COE Fellowship of Osaka University. SW acknowledges JSPS Research Fellowship.

Notes and references

1 L. W. Miller and V. W. Cornish, *Curr. Opin. Chem. Biol.*, 2005, **9**, 56.
2 (*a*) P. I. H. Bastiaens and T. M. Jovin, *Proc. Natl. Acad. Sci. U. S. A.*, 1996, **93**, 8407; (*b*) J. Yin, F. Liu, X. Li and C. T. Walsh, *J. Am. Chem. Soc.*, 2004, **126**, 7754; (*c*) I. Chen, M. Howarth, W. Lin and A. Y. Ting, *Nat. Methods*, 2005, **2**, 99; (*d*) L. W. Miller, Y. Cai, M. P. Sheetz and V. W. Cornish, *Nat. Methods*, 2005, **2**, 255; (*e*) G. Ulrich, C. Goze, M. Guardigli, A. Roda and R. Ziessel, *Angew. Chem., Int. Ed.*, 2005, **44**, 3694; (*f*) R. McRae, B. Lai, S. Vogt and C. J. Fahrni, *J. Struct. Biol.*, 2006, **155**, 22; (*g*) H.-K. Kim, J. Liu, J. Li, N. Nagraj, M. Li, C. M.-B. Pavot and Y. Lu, *J. Am. Chem. Soc.*, 2007, **129**, 6896; (*h*) B. Li, H. Wei and S. Dong, *Chem. Commun.*, 2007, 73; (*i*) B. C. Dickinson and C. J. Chang, *J. Am. Chem. Soc.*, 2008, **130**, 9638; (*j*) M. A. Brun, K.-T. Tan, E. Nakata, M. J. Hinner and K. Johnsson, *J. Am. Chem. Soc.*, 2009, **131**, 5873; (*k*) H. Ren, F. Xiao, K. Zhan, Y.-P. Kim, H. Xie, Z. Xia and J. Rao, *Angew. Chem., Int. Ed.*, 2009, **48**, 9658; (*l*) Y. Zou and J. Yin, *J. Am. Chem. Soc.*, 2009, **131**, 7548.
3 R. Y. Tsien, *Annu. Rev. Biochem.*, 1998, **67**, 509.
4 M. Fernandez-Suarez and A. Y. Ting, *Nat. Rev. Mol. Cell Biol.*, 2008, **9**, 929.
5 (*a*) B. A. Griffin, S. R. Adams and R. Y. Tsien, *Science*, 1998, **281**, 269; (*b*) C. Hoffmann, G. Gaietta, M. Bünemann, S. R. Adams, S. Oberdorff-Maass, B. Behr, J.-P. Vilardaga, R. Y. Tsien, M. H. Ellisman and M. J. Lohse, *Nat. Methods*, 2005, **2**, 171.
6 (*a*) A. Keppler, S. Gendreizig, T. Gronemeyer, H. Pick, H. Vogel and K. Johnsson, *Nat. Biotechnol.*, 2003, **21**, 86; (*b*) D. Maurel, S. Banala, T. Laroche and K. Johnsson, *ACS Chem. Biol.*, 2010, **5**, 507.
7 (*a*) H. Nonaka, S. Tsukiji, A. Ojida and I. Hamachi, *J. Am. Chem. Soc.*, 2007, **129**, 15777; (*b*) G. V. Los, L. P. Encell, M. G. McDougall, D. D. Hartzell, N. Karassina, C. Zimprich, M. G. Wood, R. Learish, R. F. Ohana, M. Urh, D. Simpson, J. Mendez, K. Zimmerman, P. Otto, G. Vidugiris, J. Zhu, A. Darzins, D. H. Klaubert, R. F. Bulleit and K. V. Wood, *ACS Chem. Biol.*, 2008, **3**, 373.
8 (*a*) M. W. Popp, J. M. Antos, G. M. Grotenbreg, E. Spooner and H. L. Ploegh, *Nat. Chem. Biol.*, 2007, **3**, 707; (*b*) H. Baruah, S. Puthenveetil, Y. A. Choi, S. Shah and A. Y. Ting, *Angew. Chem., Int. Ed.*, 2008, **47**, 7018.
9 H. Kobayashi, M. Ogawa, R. Alford, P. L. Choyke and Y. Urano, *Chem. Rev.*, 2010, **110**, 2620.
10 S. Mizukami, S. Watanabe, Y. Hori and K. Kikuchi, *J. Am. Chem. Soc.*, 2009, **131**, 5016.
11 G. Guillaume, M. Vanhove, J. Lamotte-Brasseur, P. Ledent, M. Jamin, B. Joris and J.-M. Frère, *J. Biol. Chem.*, 1997, **272**, 5438.
12 H. Adachi, T. Ohta and H. Matsuzawa, *J. Biol. Chem.*, 1991, **266**, 3186.
13 R. Livingston, L. Thompson and M. V. Ramarao, *J. Am. Chem. Soc.*, 1952, **74**, 1073.
14 Y. Hori, H. Ueno, S. Mizukami and K. Kikuchi, *J. Am. Chem. Soc.*, 2009, **131**, 16610.
15 T. Maier and W. Pfleiderer, *Nucleosides, Nucleotides Nucleic Acids*, 1995, **14**, 961.
16 (*a*) M. E. Germain, T. R. Vargo, B. A. McClure, J. J. Rack, P. G. Van Patten, M. Odoi and M. J. Knapp, *Inorg. Chem.*, 2008, **47**, 6203; (*b*) J.-S. Yang and T. M. Swager, *J. Am. Chem. Soc.*, 1998, **120**, 5321.
17 (*a*) E. L. Kapinus and I. I. Dilung, *Chem. Phys. Lett.*, 1990, **174**, 75; (*b*) K.-S. Focsaneanu and J. C. Scaiano, *Photochem. Photobiol. Sci.*, 2005, **4**, 817; (*c*) H. Li, J. Kang, L. Ding, F. Lu and Y. Fang, *J. Photochem. Photobiol., A*, 2008, **197**, 226.

J|A|C|S COMMUNICATIONS

Published on Web 06/29/2010

Photocontrolled Compound Release System Using Caged Antimicrobial Peptide

Shin Mizukami,[†,‡] Mariko Hosoda,[†] Takafumi Satake,[†] Satoshi Okada,[†] Yuichiro Hori,[†] Toshiaki Furuta,[§] and Kazuya Kikuchi*[,†,‡]

Division of Advanced Science and Biotechnology, Graduate School of Engineering, and Immunology Frontier Research Center, Osaka University, Osaka 565-0871, Japan, and Department of Biomolecular Science and Research Center for Materials with Integrated Properties, Toho University, Chiba 274-8510, Japan

Received March 15, 2010; E-mail: kkikuchi@mls.eng.osaka-u.ac.jp

Abstract: A novel photocontrolled compound release system using liposomes and a caged antimicrobial peptide was developed. The caged antimicrobial peptide was activated by UV irradiation, resulting in the formation of pores on the liposome surface to release the contained fluorophores. The compound release could be observed using fluorescence measurements and time-lapse fluorescence microscopy. UV irradiation resulted in a quick release of the inclusion compounds (within 1 min in most cases) under simulated physiological conditions. The proposed system is expected to be applicable in a wide range of fields from cell biology to clinical sciences.

Caged compounds are photoactivatable probes that are biologically or functionally inert prior to their uncaging. Photoactivation of a caged compound enables the spatiotemporal regulation of various biomolecules of interest in living cells or tissues. Thus, photoactivation technologies using caged compounds have been used as powerful tools in recent biological studies. Various caged compounds such as Ca^{2+}, neurotransmitters, nucleotides, peptides, and enzymes have been reported thus far.[1] Caged compounds provide biologists with valuable tools for investigating biological phenomena. However, current caging/uncaging systems require the synthesis of individual caged compounds for each target biomolecule. Because such syntheses generally entail complicated and multistep reactions, the development of a new methodology is desired for enabling the widespread use of photoactivation technology that can be applicable to various biomolecules ranging from small molecules to macromolecules such as proteins and nucleic acids.

We presume that a nano- or microscale photodegradable "cage" can be used for this purpose. This photoactivation system is essentially similar to the controlled drug release systems investigated from a clinical perspective.[2] Among the various drug carriers, liposomes have been actively developed;[3] further, various types of photoinduced drug-releasing liposomes have been reported. Such functional liposomes generally consisted of designed lipids such as photoisomeric lipids[4] or photocaged lipids.[5] Very recently, photoinduced drug release systems using photocaged dendrons[6] or polymeric microcapsules functionalized with bacteriorhodopsin[7] have also been reported. Nevertheless, the development of a new and practical photocontrolled release system is still strongly required. In this paper, we report a novel photocontrolled release system that works on the basis of a strategy that is clearly different from previously known strategies.

In our proposed system, a photoresponsive drug carrier was divided into two parts: a drug carrier and a photoresponsive opener.

Chart 1. Structures of TL and BTL

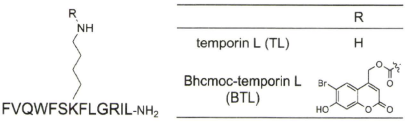

We selected liposomes as the drug carriers because of their versatility and biocompatibility. While selecting the photoresponsive opener, we focused on the membrane-damaging properties of antimicrobial peptides (AMPs).[8] AMPs have attracted increasing attention as a new category of antibiotics. In natural systems, AMPs target the lipid bilayers of bacterial membranes and kill the bacteria by disrupting their membranes. AMPs also degrade liposomes whose compositions are similar to those of the bacterial membrane. Therefore, we assumed that this membrane-damaging property can be applied to construct a photocontrolled drug release system.

We designed a protected AMP derivative Bhcmoc-temporin L (BTL) (Chart 1). BTL consists of a short antimicrobial peptide temporin L (TL),[8b,c] which was isolated from the European red frog *Rana temporaria*, and a photoremovable 6-bromo-7-hydroxycoumarin-4-ylmethyloxycarbonyl (Bhcmoc) group.[9] The Bhcmoc group was attached to the ε-amino group of the Lys. The positively charged amino acid residues of AMPs play important roles in the bacterial membrane damaging properties of AMPs.[8] Thus, protective modification of the Lys in TL was expected to reduce its membrane damaging properties. It was assumed that after the protective group was removed using UV irradiation, its membrane damaging properties would be recovered. As shown in Figure 1, we expected that the combination of BTL and a liposome having the same lipid composition as the bacterial outer membranes would provide a UV-responsive drug release system.

BTL was synthesized in the following two steps: solid-phase Fmoc peptide synthesis and subsequent modification of the Bhcmoc group (Scheme S1 in the Supporting Information). All the synthetic procedures were performed on resins, and the final product was

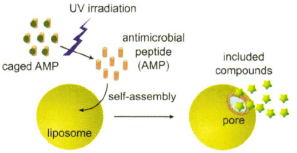

Figure 1. Schematic diagram of photocontrolled release system using caged antimicrobial peptide.

[†] Division of Advanced Science and Biotechnology, Graduate School of Engineering, Osaka University.
[‡] Immunology Frontier Research Center, Osaka University.
[§] Toho University.

10.1021/ja102167m

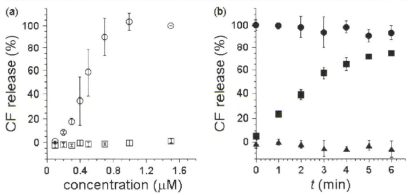

Figure 2. CF release from LUVs induced by synthesized compounds. Lipid concentration: 2.5 μg/mL. Error bars indicate the SD ($n = 3$). (a) Correlation between CF release and concentration of compounds (circles: TL, squares: BTL) under dark conditions. (b) Correlation between CF release and UV irradiation time t in the presence of 4 μM compounds (circles: TL, squares: BTL, triangles: none).

purified by reversed-phase HPLC after the cleavage from the resin and was identified by ESI-TOF MS.

The UV-light-induced conversion of BTL to TL was confirmed using HPLC analysis. Over 95% of BTL underwent conversion within 5 min of UV irradiation; simultaneously a few new peaks emerged in the HPLC analysis (Figure S1 in the Supporting Information). One of these new peaks was assigned to TL. Thus, it was confirmed that BTL was converted to TL using UV light.

Next, we examined whether or not the membrane-damaging property of TL was nullified by the modification of the Lys residue with the Bhcmoc group. Liposomes containing fluorescence dyes have been utilized as a standard tool for the evaluation of the membrane-damaging activities of AMPs and their mimics.[10] When the AMPs disrupt the lipid membrane of the liposomes, the dyes in the liposomes are released. We prepared large unilamellar vesicles (LUVs) and 5(6)-carboxyfluorescein (CF) as the encapsulated fluorescence dye. Since the fluorescence of CF in LUVs is partly quenched because of the high concentration effect, the collapse of the LUV membrane induces the increase in the fluorescence. A fraction of the release activity was estimated using this increase in the fluorescence. As shown in Figure 2a, addition of TL induced the release of CF with a concentration in the submicromolar range. In contrast, BTL did not induce the leakage of CF with a several micromolar concentration. These results indicate that the modification of the Bhcmoc group at the Lys of TL drastically reduced its membrane damaging property. In addition, CD spectra of TL and BTL showed that substitution at the Lys negatively affects the α-helix formation in the presence of liposomes (Figure S2 in the Supporting Information).

Next, the photocontrolled release of CF from LUVs was examined by using BTL and applying UV irradiation. LUV solutions were irradiated using a UV lamp for various periods of time in the presence or absence of BTL. The lamp was then switched off for 60 s, after which the fluorescence intensities of the sample were measured. In the presence of BTL, a fraction of the CF release was dependent on the UV exposure time (Figure 2b). UV irradiation in the absence of BTL did not induce CF release. Thus, photocontrolled release was achieved by the appropriate adjustment of the BTL concentration and UV exposure time.

Finally, the applicability of the photocontrolled release system to fluorescence microscopic studies was examined. Giant unilamellar vesicles (GUVs) were selected for this purpose, because GUVs have larger diameters and the changes in their shape can be observed using optical microscopes. Prepared GUVs containing CF were loaded on a poly-L-lysine-coated glass-bottom dish and observed using a fluorescence microscopic imaging system. The fluorescence images were captured by the excitation of visible light ($\lambda = 460-490$ nm). The

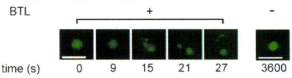

Figure 3. Fluorescence microscopic images of GUVs containing CF under UV irradiation in the presence (12.5 μM) or absence of BTL. Scale bar: 10 μm.

GUVs were stable for several hours under the experimental conditions. When 12.5 μM TL was added, the fluorescence of the GUVs completely disappeared within 40 s, although the addition of 12.5 μM BTL did not induce the disruption of GUVs (data not shown). The GUVs were then irradiated by UV light ($\lambda = 330-385$ nm) using a fluorescence microscope. In the absence of BTL, the GUVs were stable under the microscopic UV excitation. On the other hand, in the presence of BTL, leakage of the CF from the GUVs mostly with the membrane blebbing was observed within tens of seconds under the UV irradiation (Figure 3). In most cases, the leakage was completed within 1 min.

In conclusion, we developed a novel photocontrolled release system by combining liposomes and a caged antimicrobial peptide. This system was experimentally found to be effective for liposomes of different sizes. The response to UV irradiation was rapid, and the release was induced under simulated physiological conditions and also under the experimental conditions of time-lapse fluorescence microscopy. These data imply that this system could be applicable to fluorescence imaging for living cells or living animals. Because liposomes tolerate a wide variety of inclusion compounds from small molecules to macromolecules, this system could enable the development of a universal photouncaging system that might offer a breakthrough in biological studies. Further, in terms of clinical applications, this technology might be applied to other external stimuli such as specific enzyme activities in diseased tissues. This controlled release system may be useful in a wide range of research fields from cell biology to clinical medicine.

Acknowledgment. We thank Drs. Shigenori Kanaya and Yuichi Koga at Osaka University for the use of CD spectrometer. This work was supported in part by MEXT of Japan. S.M. thanks the Cosmetology Research Foundation.

Supporting Information Available: Detailed experimental procedures and supplementary results. This material is available free of charge via the Internet at http://pubs.acs.org.

References

(1) Mayer, G.; Heckel, A. *Angew. Chem., Int. Ed.* **2006**, *45*, 4900–4921.
(2) (a) Rapoport, N. *Prog. Polym. Sci.* **2007**, *32*, 962–990. (b) Shum, P.; Kim, J.-M.; Thompson, D. H. *Adv. Drug Delivery Rev.* **2001**, *53*, 273–284. (c) Chilkoti, A.; Dreher, M. R.; Meyer, D. E.; Raucher, D. *Adv. Drug Delivery Rev.* **2002**, *54*, 613–630. (d) Schmaljohann, D. *Adv. Drug Delivery Rev.* **2008**, *58*, 1655–1670.
(3) Torchilin, V. P. *Nat. Rev. Drug Discov.* **2005**, *4*, 145–160.
(4) (a) Bisby, R. H.; Mead, C.; Morgan, C. G. *Biochem. Biophys. Res. Commun.* **2000**, *276*, 169–173. (b) Liu, X.-M.; Yang, B.; Wang, Y. L.; Wang, J.-Y. *Chem. Mater.* **2005**, *17*, 2792–2795.
(5) (a) Zhang, Z.-Y.; Smith, B. D. *Bioconjugate Chem.* **1999**, *10*, 1150–1152. (b) Watanabe, S.; Hiratsuka, R.; Kasai, Y.; Munakata, K.; Takahashi, Y.; Iwamura, M. *Tetrahedron* **2002**, *58*, 1685–1691. (c) Chandra, B.; Subramaniam, R.; Mallik, S.; Srivastava, D. K. *Org. Biomol. Chem* **2006**, *4*, 1730–1740.
(6) Park, C.; Lim, J.; Yun, M.; Kim, C. *Angew. Chem., Int. Ed.* **2008**, *47*, 2959–2963.
(7) Erokhina, S.; Benassi, L.; Bianchini, P.; Diaspro, A.; Erokhin, V.; Fontana, M. P. *J. Am. Chem. Soc.* **2009**, *131*, 9800–9804.
(8) (a) Zasloff, M. *Nature* **2002**, *415*, 389–395. (b) Mahalka, A. K.; Kinnunen, P. K. J. *Biochim. Biophys. Acta* **2009**, *1788*, 1600–1609. (c) Rinaldi, A. C.; Mangoni, M. L.; Rufo, A.; Luzi, C.; Barra, D.; Zhao, H.; Kinnunen, P. K. J.; Bozzi, A.; Giulio, A. D.; Simmaco, M. *Biochem. J.* **2002**, *368*, 91–100.
(9) (a) Furuta, T.; Wang, S. S.; Dantzker, J. L.; Dore, T. M.; Bybee, W. J.; Callaway, E. M.; Denk, W.; Tsien, R. Y. *Proc. Natl. Acad. Sci. U.S.A.* **1999**, *96*, 1193–1200. (b) Ando, H.; Furuta, T.; Tsien, R. Y.; Okamoto, H. *Nat. Genet.* **2001**, *28*, 317–325. (c) Furuta, T.; Watanabe, T.; Tanabe, S.; Sakyo, J.; Matsuda, C. *Org. Lett.* **2007**, *9*, 4717–4720.
(10) Tew, G. N.; Liu, D.; Chen, B.; Doerksen, R. J.; Kaplan, J.; Carroll, P. J.; Klein, M. L.; DeGrado, W. F. *Proc. Natl. Acad. Sci. U.S.A.* **2002**, *99*, 5110–5114.

JA102167M

DOI: 10.1002/cbic.201100021

Cell-Surface Protein Labeling with Luminescent Nanoparticles through Biotinylation by Using Mutant β-Lactamase-Tag Technology

Akimasa Yoshimura,[a] Shin Mizukami,[a, b] Yuichiro Hori,[a] Shuji Watanabe,[a] and Kazuya Kikuchi*[a, b]

Cell-surface proteins play important roles in various biological processes. Most of these proteins are classified into groups on the basis of their functions, such as membrane receptors, ion channels, or transporters. These proteins transduce biological signals in response to extracellular signals or transport biological substances from outside cells to their interiors. It is therefore important to investigate the activities and localization of cell-surface proteins. Fluorescence imaging with luminescent quantum dots (QDs) as fluorophores is an established surface protein identification method.[1] QDs are semiconductor nanoparticles with many unique attributes, such as stronger emission intensities than small molecular dyes and remarkable resistance to photobleaching. QDs can simultaneously display different colors when excited by a single wavelength, so multicolor imaging can be achieved through simple experiments. Labeling of cell-surface proteins with QDs facilitates investigation of protein localization, movement, and so on.

To introduce QDs onto proteins of interest (POIs), biotinylation was exploited, because biotin binds strongly to commercially available streptavidin-conjugated QDs. Biotinylation of POIs has thus enabled the introduction of various kinds of QDs onto proteins. Previously, modification of QDs through biotinylation has been performed with a biotin ligase[2] or a Halo-tag.[3] In addition, other protein-labeling methods using tag proteins,[4] tag peptides,[5] or enzymes[6] are applicable.

We recently developed a novel protein-labeling system based on the use of mutant β-lactamase (BL-tag) and low-molecular-weight fluorescent β-lactam probes that involve turn-on fluorescence switches based on FRET[7] or aggregation quenching.[8] The fluorophores on these probes are small fluorescent molecules, such as fluorescein, which are prone to photobleaching. For multicolor fluorescence imaging, we synthesized probes of various colors and applied other protein-labeling techniques. On the other hand, POIs can be labeled with streptavidin-conjugated functional molecules, for instance MRI contrast agents, by biotinylation. We therefore report here a novel biotinylation probe for the BL-tag and demonstrate its application in multicolor labeling with use of streptavidin-conjugated QDs that are resistant to photobleaching. With this system, pulse-chase labeling of cell-surface protein was achieved easily because we used different QDs for the same POIs with different expression timing (Scheme 1).

The labeling activity of BHA for BL-tag was confirmed. Purified BL-tag protein was incubated with BHA in Tris·HCl buffer (pH 7.0, 10 mM) at 25 °C and then analyzed by Western blot. The biotinylated protein, which was detected by use of streptavidin-horseradish peroxidase (HRP) and its substrate, were observed at ~29 kDa (Figure 1A). The reaction rate of BHA and BL-tag protein was then investigated from the time course of the band signal in the Western blot (Figure 1B). The reaction had gone to completion within 60 min under the reaction conditions.

QDs labeling of a cell-surface protein was performed. Cell-surface proteins fused with BL-tag at their extracellular termini can be labeled with BHA and streptavidin-conjugated QDs. We selected epidermal growth factor receptor (EGFR) as the POI because EGFR is known to be overexpressed in several types of cancers, such as lung or stomach cancer.[9] It was also reported that internalization of EGFR transduces the cell proliferation signals to intracellular milieu. EGFR fused with the BL-tag at the N terminus (BL-EGFR) was overexpressed on the plasma membranes of mammalian HEK293T cells. BL-EGFR was then labeled with QD605 ($\lambda_{em,max}$ = 605 nm) in two steps with use of BHA and streptavidin-conjugated QD605. When the cells were observed under a confocal laser scanning microscope, only the cells overexpressing BL-EGFR showed red fluorescence from the plasma membranes (Figure 2A). No fluorescence was observed from the plasma membranes of the cells overexpressing EGFR. One-step QDs labeling was also performed. BHA was mixed with QD605 to form the BHA-QDs conjugate before incubation with HEK293T cells. As a result, QD605 fluorescence was detected from the plasma membranes of the cells overexpressing BL-EGFR (Figure S1 in the Supporting Information).

Resistance to photobleaching of the QDs was next compared with the previously reported value for the fluorescein-based probe FA.[7b] FA is an ampicillin-based fluorescent probe that contains carboxy fluorescein and can directly bind to BL-tag (Figure S2A). QD605 and FA were labeled on BL-EGFR overexpressed on HEK293T cells, and the labeled cells were then irradiated 16 times at 3 min intervals under a confocal laser fluorescence microscope. The fluorescence of QD605 was stable and allowed long-term imaging. On the other hand, FA was gradually bleached by repeated excitation (Figure S2B). The time course of the averaged fluorescence intensity in the field of view clearly indicates that QD605 was more resistant to photobleaching than FA (Figure S2C).

Imaging of EGFR internalization was next performed. It is well known that stimulation by epidermal growth factor (EGF) induces migration of cell surface EGFR into cytosol as a component of endosomal vesicles. This internalization is an impor-

[a] A. Yoshimura, Dr. S. Mizukami, Dr. Y. Hori, S. Watanabe, Prof. K. Kikuchi
Graduate School of Engineering, Osaka University
Osaka 565-0871 (Japan)
Fax: (+81) 6-6879-7924
E-mail: kkikuchi@mls.eng.osaka-u.ac.jp

[b] Dr. S. Mizukami, Prof. K. Kikuchi
Immunology Frontier Research Center (IFReC), Osaka University
Osaka 565-0871 (Japan)

Supporting information for this article is available on the WWW under http://dx.doi.org/10.1002/cbic.201100021.

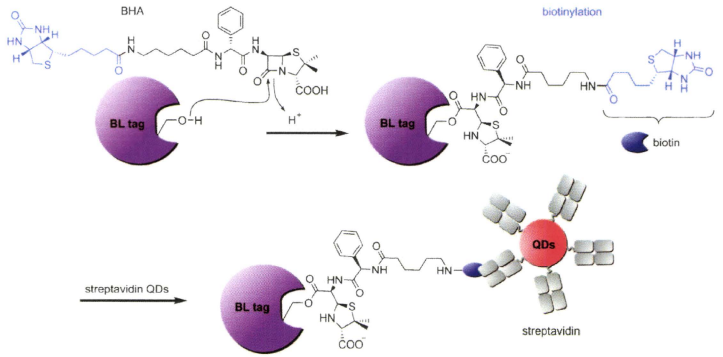

Scheme 1. Structure of the biotin-labeling probe (BHA) and labeling mechanism.

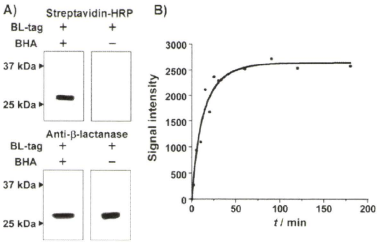

Figure 1. A) Western blot of BL-tag incubated with BHA. Protein bands were visualized by use of streptavidin-conjugated HRP (top) and anti-β-lactamase antibody (bottom). B) Binding reaction rate of BHA (2 μM) and BL-tag (1 μM) at RT in Tris-HCl buffer (pH 7.0, 10 mM). Aliquots of the solution mixture were analyzed at the indicated time points. The signal intensities were determined from the bands in Western blot.

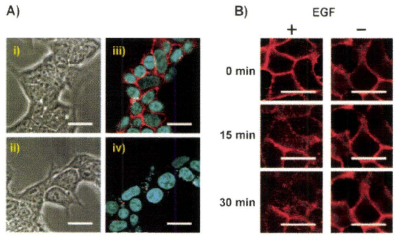

Figure 2. A) Labeling of EGFR on surfaces of HEK293T cells. The cells were costained with Hoechst 33342. Scale bar: 20 μm. Phase-contrast microscopic images of the cells expressing i) BL-EGFR, and ii) EGFR. Fluorescence microscopic images of the cells expressing iii) BL-EGFR, and iv) EGFR. B) Time-lapse fluorescence imaging of the internalization of BL-EGFR labeled with QD605-streptavidin by stimulation of EGF (100 ng mL^{-1}). Scale bar = 20 μm.

tant process for EGFR-mediated signal transduction. Although many studies on the imaging of EGFR internalization have been reported, by use of a GFP-EGFR fusion protein,[10] a fluorescently labeled EGF,[11] or anti-EGFR antibody,[12] there are few reports in which cell-surface proteins have been labeled by QDs. Figure 2B shows time-lapse imaging of the EGF-induced internalization of BL-EGFR labeled with QD605 in living HEK293T cells. Before stimulation by EGF, QD605 fluorescence was localized at the cell surfaces. The fluorescent portions were gradually internalized into the cytoplasmic regions upon stimulation with EGF (100 ng mL^{-1}). In the absence of stimulation, no such dynamic fluorescence change was observed within 30 min.

The pulse-chase imaging of EGFR in living HEK293T cells was then performed with the aid of BHA and three different QDs. BL-EGFR was labeled with QD605, QD525, and QD655 18, 24, and 30 h after transfection, respectively (Figure 3A). The purpose of this experiment was to label newly expressed protein with different kinds of QDs and to visualize the time-dependent localization changes, induced by a small amount of EGF included in the fetal bovine serum (FBS). BL-EGFR expressed in the first 18 h after transfection was selectively visualized as red fluorescence, whereas the proteins expressed 18–24 h and 24–30 h after transfection were labeled in the other fluorescence colors, which are shown as green and blue, respectively, in Figure 3B. Although fluorescence of QDs was mostly detected from the plasma membrane immediately after labeling, some of them were internalized and fluorescent vesicles could be detected inside cells 6 h after labeling. From the merged fluorescence images of different QDs, red and green fluorescent dots can be recognized, so we can distinguish the internalized EGFRs from the newly expressed EGFRs. As a result, pulse-

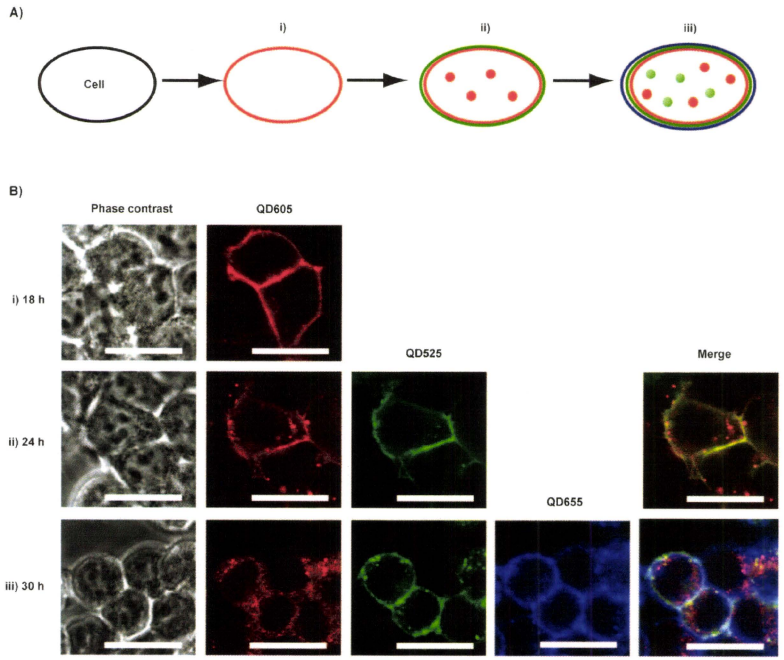

Figure 3. A) Schematic representation of the pulse-chase labeling of BL-EGFR labeled with three QDs. B) Fluorescence images of QDs-labeled BL-EGFR i) 18, ii) 24, and iii) 30 h after transfection. Scale bar = 20 μm.

chase imaging of EGFR was successful with feasible experimental setups with BL-tag and QDs; these experiments are not successful with use of fluorescent proteins. Imaging was successful with a single excitation laser and a single expressed protein, so the photochemical characteristics of the QDs were well suited for monitoring the timing of protein expression.

In conclusion, we have developed a novel biotinylation probe, BHA, and have demonstrated its application in fluorescence imaging of POIs on living cell surfaces. EGFR fused with BL-tag was selectively biotinylated and successively labeled with various colors of QD through streptavidin–biotin binding. Our previous labeling method, based on small-molecular fluorescent probes, was modified for use with BHA. Because QDs are more resistant to photobleaching than the fluorescein-based probe, this technology should be useful for experiments that require strong excitation. This method was also applicable to time-lapse fluorescence imaging of EGFR internalization. Moreover, we successfully labeled proteins at different expression times on cell surfaces with three different colors of QD. This pulse-chase labeling is a powerful method for studying dynamic cellular processes, such as biological structure formation. Furthermore, if near-infrared-fluorescent QDs are used, this method can be applied to in vivo imaging studies. These versatile properties of the biotin-labeling technology should allow studies of various protein functions and lead to the development of new drugs or therapeutic approaches.

Experimental Section

Detailed experimental procedures for the synthesis and characterization of all compounds, as well as a detailed description of all experiments, are given in the Supporting Information.

Acknowledgements

This work was supported in part by a Grant-in-Aid for Scientific Research from the Ministry of Education, Culture, Sports, Science

and Technology (MEXT) of Japan, by a Grant-in-Aid from the Ministry of Health, Labor, and Welfare (MHLW) of Japan, by the Funding Program for World-Leading Innovative R&D on Science and Technology from the Japan Society for the Promotion of Science (JSPS), and by the Japan Science and Technology Agency Core Research for Evolutional Science and Technology (JST CREST).

Keywords: biotinylation · epidermal growth factor receptor · fluorescence · mutant beta-lactamase · quantum dots

[1] X. Michalet, F. F. Pinaud, L. A. Bentolia, J. M. Tsay, S. Doose, J. J. Li, G. Sundaresan, A. M. Wu, S. S. Gambhir, S. Weiss, *Science* **2005**, *307*, 538–544.

[2] M. Howarth, K. Takao, Y. Hayashi, A. Y. Ting, *Proc. Natl. Acad. Sci. USA* **2005**, *102*, 7583–7588.

[3] M. K. So, H. Yao, J. Rao, *Biochem. Biophys. Res. Commun.* **2008**, *374*, 419–423.

[4] a) G. V. Los, L. P. Encell, M. G. McDougall, D. D. Hartzell, N. Karassina, C. Zimprich, M. G. Wood, R. Learish, R. F. Ohana, M. Urh, D. Simpson, J. Mendez, K. Zimmerman, P. Otto, G. Vidugiris, J. Zhu, A. Darzins, D. H. Klaubert, R. F. Bulleit, K. V. Wood, *ACS Chem. Biol.* **2008**, *3*, 373–382; b) A. Keppler, S. Gendreizig, T. Gronemeyer, H. Pick, H. Vogel, K. Johnsson, *Nat. Biotechnol.* **2002**, *21*, 86–89; c) S. S. Gallagher, J. E. Sable, M. P. Sheetz, V. W. Cornish, *ACS Chem. Biol.* **2009**, *4*, 547–556.

[5] a) B. A. Griffin, S. R. Adams, R. Y. Tsien, *Science* **1998**, *281*, 269–272; b) A. Ojida, K. Honda, D. Shinmi, S. Kiyonaka, Y. Mori, I. Hamachi, *J. Am. Chem. Soc.* **2006**, *128*, 10452–10459; c) C. T. Hauser, R. Y. Tsien, *Proc. Natl. Acad. Sci. USA* **2007**, *104*, 3693–3697.

[6] a) I. Chen, M. Howarth, W. Lin, A. Y. Ting, *Nat. Methods* **2005**, *2*, 99–104; b) N. George, H. Pick, H. Vogel, N. Johnsson, K. Johnsson, *J. Am. Chem. Soc.* **2004**, *126*, 8896–8897.

[7] a) S. Mizukami, S. Watanabe, Y. Hori, K. Kikuchi, *J. Am. Chem. Soc.* **2009**, *131*, 5016–5017; b) S. Watanabe, S. Mizukami, Y. Hori, K. Kikuchi, *Bioconjugate Chem.* **2010**, *21*, 2320–2326.

[8] K. K. Sadhu, S. Mizukami, S. Watanabe, K. Kikuchi, *Chem. Commun.* **2010**, *46*, 7403–7405.

[9] a) Q. Wang, G. Villeneuve, Z. Wang, *EMBO Rep.* **2005**, *6*, 942–948; b) D. L. Wheeler, E. F. Dunn, P. M. Harari, *Nat. Rev. Clin. Oncol.* **2010**, *7*, 493–507.

[10] R. E. Carter, A. Sorkin, *J. Biol. Chem.* **1998**, *273*, 35000–35007.

[11] a) R. Brock, R. B. Hamelers, T. M. Jovin, *Cytometry* **1999**, *35*, 353–362; b) D. S. Lidke, P. Nagy, R. Heintzmann, D. J. A. Jovin, J. N. Post, H. E. Grecco, E. A. J. Erijman, T. M. Jovin, *Nat. Biotechnol.* **2004**, *22*, 198–203.

[12] a) Q. Yuan, E. Lee, W. A. Yeudall, H. Yang, *Oral Oncol.* **2010**, *46*, 698–704; b) J. Lee, Y. Choi, K. Kim, S. Hong, H. Y. Park, T. Lee, G. J. Cheon, R. Song, *Bioconjugate Chem.* **2010**, *21*, 940–946; c) H. Xu, P. K. Eck, K. E. Baidoo, P. L. Choyke, M. W. Brechbiel, *Bioorg. Med. Chem.* **2009**, *17*, 5176–5181.

Received: January 12, 2011
Published online on March 18, 2011

Molecular BioSystems

View Online
Dynamic Article Links

Cite this: *Mol. BioSyst.*, 2011, **7**, 1766–1772

www.rsc.org/molecularbiosystems

PAPER

Sequential ordering among multicolor fluorophores for protein labeling facility *via* aggregation-elimination based β-lactam probes†

Kalyan K. Sadhu,[a] Shin Mizukami,[ab] Shuji Watanabe[a] and Kazuya Kikuchi*[ab]

Received 12th January 2011, Accepted 24th February 2011
DOI: 10.1039/c1mb05013c

Development of protein labeling techniques with small molecules is enthralling because this method brings promises for triumph over the limitations of fluorescent proteins in live cell imaging. This technology deals with the functionalization of proteins with small molecules and is anticipated to facilitate the expansion of various protein assay methods. A new straightforward aggregation and elimination-based technique for a protein labeling system has been developed with a versatile emissive range of fluorophores. These fluorophores have been applied to show their efficiency for protein labeling by exploiting the same basic principle. A genetically modified version of class A type β-lactamase has been used as the tag protein (BL-tag). The strength of the aggregation interaction between a fluorophore and a quencher plays a governing role in the elimination step of the quencher from the probes, which ultimately controls the swiftness of the protein labeling strategy. Modulation in the elimination process can be accomplished by the variation in the nature of the fluorophore. This diversity facilitates the study of the competitive binding order among the synthesized probes toward the BL-tag labeling method. An aggregation and elimination-based BL-tag technique has been explored to develop an order of color labeling from the equimolar mixture of the labeling probe in solutions. The qualitative and quantitative determination of ordering within the probes toward labeling studies has been executed through SDS-PAGE and time-dependent fluorescence intensity enhancement measurements, respectively. The desirable multiple-wavelength fluorescence labeling probes for the BL-tag technology have been developed and demonstrate broad applicability of this labeling technology to live cell imaging with coumarin and fluorescein derivatives by using confocal microscopy.

Introduction

In recent years, research with photosensitive molecular probes possessing high selectivity has been used for analyzing cellular processes with several potential applications.[1] The use of genetically encoded fluorescent tags has drawn attention toward the subcellular distributions of many proteins.[2] An advanced technique to bring forth photosensitive proteins is the site-specific labeling of proteins with tailor-made photosensitive small probes. Several protein mediated labeling methods such as the tetracysteine tag,[3] the HaloTag,[4] the SNAP-tag,[5] tetraaspartate,[6] α-bungarotoxin binding peptide,[7] combination of tetraserine and bisboronic acid,[8] and dihydrofolate reductase[9] are known in literature. The method based on single-chain variable fragment (scFv) antibodies and non-covalently bound fluorogenic dyes was developed.[10] Proficiency in molecular biology furnishes the development of probe designing, and this blending can enable the modification of labeling experiments. The coalescence of two orthogonal tagging methods provides access to develop new labeling experiments due to their simultaneous performance. We have recently shown simultaneous orthogonal labeling of our technique and the SNAP-tag in cell imaging studies.[11] Other reports depict the generation of fluorescent labeling techniques that can be exclusively conjugated to SNAP-tag fusion proteins.[1h,12] The choice of color for studying the dynamic processes in different domains of mammalian cells would be improvised with multifaceted fluorophores for each of the merged labeling techniques. Our current approach will be helpful to modify the technique for multicolor labeling with a genetically modified β-lactamase protein. In this present work, we have developed a new technique to determine an order of the studied probes in the labeling efficiency, which ensued from the aggregation interaction energies between the fluorophore and the quencher.

In our earlier studies we have depicted a novel protein labeling system by conglutination of genetically modified β-lactamase

[a] *Division of Advanced Science and Biotechnology, Graduate School of Engineering, Osaka University, 2-1 Yamadaoka, Suita, Osaka 565-0871, Japan. E-mail: kkikuchi@mls.eng.osaka-u.ac.jp; Web: http://www-molpro.mls.eng.osaka-u.ac.jp/; Fax: (+81) 6-6879-7875*
[b] *Immunology Frontier Research Center, Osaka University, 3-1 Yamadaoka, Suita, Osaka 565-0871, Japan*

† Electronic supplementary information (ESI) available: Experimental details, chemical structures, UV-Visible absorption spectra, and fluorescence spectra of the probes. See DOI: 10.1039/c1mb05013c.

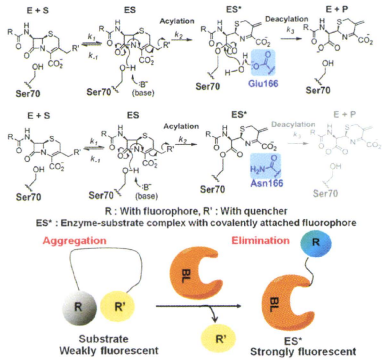

Scheme 1 Reaction mechanism of WT TEM (top) and BL-tag technique (middle) *via* control of deacylation step for protein labeling by E166N point mutation of class A β-lactamase; (E) enzyme, (S) substrate, and (P) product; general mechanism of protein labeling through covalent bond using BL-tag (bottom).

(BL-tag, Scheme 1) with low-molecular-weight fluorogenic β-lactam probes.[1e,11,13] In BL-tag technology, the acyl-enzyme intermediate (Scheme 1) is accumulated by markedly slowing the deacylation step[14] relative to the acylation step with wild-type (WT) TEM-1 (class A type β-lactamase, hereafter, WT TEM). We have successfully exploited this property of the mutant to covalently attach a fluorescent substrate with genetically modified β-lactamase for the protein labeling technique. We have also shown that the aggregation and elimination-based strategy is selectively applicable to the BL-tag labeling method.[13] Highly specific covalent labeling properties of this technology are anticipated to furnish robust tools for investigating protein functions. These probes have been ascertained to be more beneficial for fluorogenicity and specificity compared to the available green fluorescent proteins. Low invasiveness with respect to the functions of the epidermal growth factor receptor (EGFR) has been corroborated by this technique. With suitable sensitivity and swiftness of labeling, this strategy might be applicable to study protein trafficking *in vivo*.

To outstrip the limitations of our FRET-based process,[1e,11] we have recently developed a new approach based on the switching mechanism involving aggregation followed by elimination processes between a fluorophore and a quencher[13] (Scheme 1). Now, we have used this straightforward technique for the generation of controllable color variation in fluorogenic probes, with a wide range of emission wavelengths, suitable for protein labeling in living cells. The advantage of this design principle is robustness toward any fluorophore whose fluorescence intensity was not easily modified by the previous FRET-based design. In this development stage of the tailored version, we have developed a multiple color palette with different fluorophores such as coumarin, and 5- and 6-carboxyrhodamine derivatives, which support the fact that the system does not necessitate any restriction in fluorophore choice anymore as the system adopts the aggregation quenching principle. We have continued our strategy with the *m*-dinitrobenzene (DNB) group as the quencher to study the effect of aggregation interactions toward the fluorescence enhancement of the probes with a wide range of emissive fluorophores, which ultimately controls the quencher elimination step from the probe. The structures of the newly synthesized probes vary only in the fluorophoric part in our recent strategic compounds. The developed order in the BL-tag labeling efficiency of the probes is the final outcome of the moderated disaggregation steps of the probe reaction.

Results and discussion

Design and synthesis

The practical utility of the fluorescently labeled BL-tag under a physiological situation has been explored with the newly synthesized three cephalosporin-based fluorescent probes with coumarin (**CCDNB**, Scheme 2) and rhodamine isomers (**5RCDNB** and **6RCDNB**, Scheme 2). We have compared the fluorogenic nature of our new probes with a previous[13] fluorescein analog (**FCDNB**, Scheme 2).

The polyethylene glycol (PEG) spacer was used to ascertain the aggregation between the fluorophore and the quencher in each case. The PEG spacer is also beneficial for attaining a flexible structure of the probes for favorable aggregation interactions among fluorophores and quenchers. The syntheses of **CCDNB**, **5RCDNB**, and **6RCDNB** were performed using similar procedures to our earlier studies with **FCDNB**.[13] The succinimidyl ester of coumarin and 5(6)-carboxytetramethyl

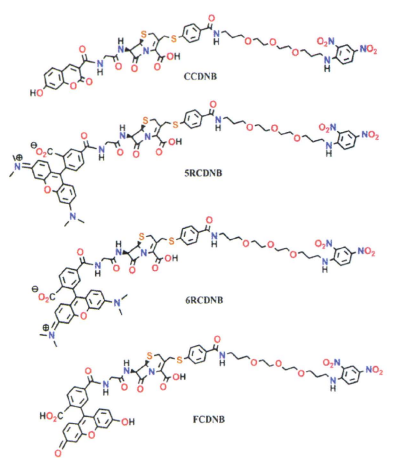

Scheme 2 Chemical structures of synthesized fluorescent probes with different colored tags for protein labeling.

rhodamine were used for corresponding probe syntheses. Final rhodamine isomeric products were separated from their mixture by preparative HPLC. The purities of all the final compounds were checked by analytical HPLC (Fig. S4–S6, ESI†), ^{1}H NMR, ^{13}C NMR, and HR-FAB-MS.

Absorption and emission studies of the free probes

Absorption studies of **CCDNB**, **5RCDNB**, and **6RCDNB** (Fig. 1) were checked in the 100 mM HEPES buffer (pH 7.4) and in methanol. The interaction between the fluorophores and the quencher is reflected in the absorption maxima of the probes in these two solvents. The maximum interaction was observed in the case of the **CCDNB** probe in the HEPES buffer. Under this physiological condition the absorption peaks of coumarin and the DNB group in **CCDNB** were obtained at 407 and 375 nm respectively. In methanol, the absorption peaks for coumarin remained at the same position, whereas the peak position of DNB was blue shifted and observed at 351 nm (Fig. S7a, ESI†). The literature reported that the absorption peak due to free *N*-ethyl-substituted 2,4-dinitroaniline[15] in methanol was quite similar to our observed value in methanol. The large shift of the DNB group with a low extinction coefficient value in an aqueous medium compared to the value reported in the literature[16] was due to the favorable aggregation interaction between coumarin and the DNB quencher in a physiological pH medium. In the case of both the rhodamine isomers, the absorption peaks of rhodamine and the DNB group were obtained at 559 and 359 nm, respectively, in the HEPES buffer. In methanol, the absorption peaks for both the DNB group and rhodamine were blue shifted by 5–15 nm (Fig. S7b, ESI†). This observation was similar to our previous finding with fluorescein derivatives in **FCDNB**.[13] The well-known capacity of the DNB group to form π-stack complexes raises the possibility that aggregation interaction of this type might contribute to the unusual stability of some fluorophore–quencher complexes.

The emission spectra of the free probes were measured in physiological pH buffer (Fig. 1) and compared with those in methanol. The fluorescence quantum yields of all the probes were significantly quenched in the 100 mM HEPES buffer (Table 1). In the aggregated form, the amount of interaction energy between the fluorogenic parts of different probes and the quencher restricts the emission of the fluorophore, which is reflected in the low quantum yield of the probes under physiological conditions. 2,4-Dinitroaniline is an efficient intramolecular fluorescence quencher for fluorophores with different emissive regions.[17] The mechanism of emission restriction might be thought to arise from the π-stacking interaction between highly electron-rich fluorophores and electron-deficient nitroaromatics. The reported electron density calculations attributing to the quenching phenomenon of the DNB group suggests electron deficiency on the DNB part.[18] Theoretical calculations involving interaction energies between the indirectly correlated groups with the DNB group confirm its legitimacy to the rational association between the substituted groups and the molecular stabilities.[19] The inherent quenching phenomenon of DNB, which does not depend upon the nature of fluorophores but rather upon the aggregation technique, has been found to be effective for several fluorogenic probes. The quantum yields of the same probes were much higher in methanol (Table 1). This significant difference in emissions in these two solutions (Fig. S8a and S8b, ESI†) implies that the aggregation phenomenon is favorable only in the aqueous buffer solution (Fig. S8c, ESI†).

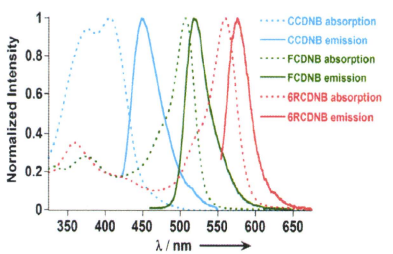

Fig. 1 Multicolor absorption and emission region involved in the aggregation-elimination strategy for BL-tag; normalized absorption and emission spectra of each probes in 100 mM HEPES buffer (pH 7.4).

Emission studies of the probes in the presence of the tag protein

To observe the fluorogenicity of the synthesized probes, the emission spectra of each probe were studied in the presence of the BL-tag and WT TEM. The reaction in the presence of WT TEM is catalytic in nature, whereas the BL-tag reaction is non-catalytic. In the presence of the BL-tag, the quencher part was eliminated from the **CCDNB** probe according to our recently developed strategy.[13] This elimination process was reflected in the fluorescence enhancement of the coumarin probe in the course of the reaction between the probe and the BL-tag with time (Fig. 2a). The fluorescence intensity at 450 nm due to coumarin (λ_{ex} = 407 nm) was monitored (Fig. 2b) after the incubation of BL-tag with **CCDNB**. In the case of both the rhodamine isomers, the monitored emission wavelength was 575 nm (λ_{ex} = 558 nm) (Fig. 2c and d). Significantly different enhancement rates of fluorescence intensities were observed with time for different fluorophoric parts in successive probes (Fig. 3b–d). The elimination step for each probe was similar in nature as the DNB quencher was used in all cases. The difference in the fluorescence enhancement rate indicates that the amount of aggregation energy between the fluorophores and the quencher is different in each case due to the accessibility of different fluorophores in the probes to the enzyme active site and this interaction curtails the next step involving disaggregation followed by elimination of the DNB group. The aggregation interaction is governed by the electron density as well as the steric bulk of the fluorophore and the quencher part, which is expected to vary with the nature of the fluorophore, as the quencher remains the same for all studied probes. Substantial increase in the fluorescence enhancement rate is observed in the case of the incubation study with WT TEM compared

Table 1 Fluorescence quantum yields of the synthesized probes in physiological pH buffer and in methanol

Solvent	Fluorescence quantum yield			
	CCDNB	**5RCDNB**	**6RCDNB**	**FCDNB**[13]
100 mM HEPES buffer (pH 7.4)	0.04	0.04	0.06	0.05
Methanol	0.19	0.24	0.25	0.42

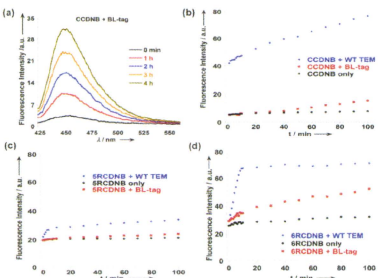

Fig. 2 (a) Time-dependent emission spectra (λ_{ex} = 407 nm) of **CCDNB** (conc. of **CCDNB**: 1.0 μM) in the presence of BL-tag in 100 mM HEPES buffer (pH 7.4) containing 0.1% DMSO at 25 °C. (b–d) Change in fluorescence intensities of (b) **CCDNB** (conc. of **CCDNB**: 1.0 μM, and λ_{ex} = 407 nm), (c) **5RCDNB** (conc. of **5RCDNB** 0.5 μM and λ_{ex} = 558 nm) and (d) **6RCDNB** (conc. of **6RCDNB**: 0.5 μM, and λ_{ex} = 558 nm) with time.

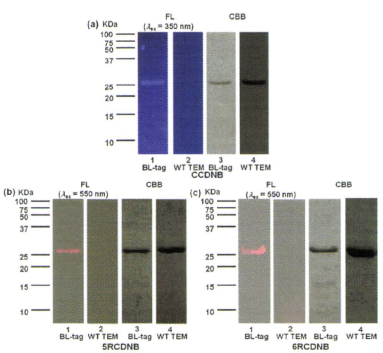

Fig. 3 Fluorescence (1 and 2) and CBB-stained (3 and 4) gel images of BL-tag and WT TEM β-lactamase incubated with (a) **CCDNB**, (b) **5RCDNB**, and (c) **6RCDNB**.

to BL-tag (Fig. 2) for all the probes as the reaction with WT TEM is catalytic in nature. The DNB group was eliminated by WT TEM at a faster rate, and the fluorescence signal increased as expected due to the favorable deacylation step in the catalytic mechanism. However, the enhancements in the fluorescence intensities in the case of different probes are not the same even in the presence of WT TEM. In the case of incubation of WT TEM with the probe **CCDNB**, 36% of the reaction was completed within 1 min, whereas in other cases this process was not so fast. Controlled elimination processes were observed when different probes with varying fluorophores were used, and the aggregation interaction between the fluorophore and the quencher is the guiding factor for such regulation. The initial rates of fluorescence enhancement in the case of WT TEM for all the probes were found to be much higher compared to the initial rates for the BL-tag. This noticeable difference in the reaction rates is mainly due to the combination of the controlled acylation path[20] and the ineffective catalytic deacylation step as a result of mutation at Glu166 of WT TEM.

Protein labeling *in vitro*

Incubation with the BL-tag protein leads to the subsequent elimination of the quencher in each probe and covalent modification of the tag protein with the desired color fluorophore. To check the versatile range of color monitoring *via* this method, SDS-PAGE studies were performed with coumarin- and rhodamine-based fluorogenic probes. The labeled protein was detected in each case by irradiating the gel with UV light (λ = 350 nm) for **CCDNB** and with visible light (λ = 550 nm) for **5RCDNB** and **6RCDNB** (Fig. 3). The corresponding labeled protein band of ~29 kDa was observed in each case. In these cases, similar experiments with WT TEM resulted in no labeled fluorescence in any case due to the lack of covalent linkage between the enzyme and the probe after the favorable deacylation step.

Qualitative ordering of labeling efficiencies of the probes

The only difference among the structures of probes is the nature of fluorophores. To check the possibility of different kinetic rates of protein labeling among the probes, several experiments were carried out. The control of the elimination step for different probes depends upon the aggregation interactions, which led to further studies to observe the effect of fluorophore in protein labeling by this new strategy. SDS-PAGE studies were carried out in several batches with the binary mixture of probes in an equimolar amount to show any preferential order of fluorophore labeling toward the BL-tag technique *via* the aggregation-elimination technique. The competitive labeling kinetics cannot distinguish between the two different kinetics steps involved: covalent interaction with the BL-tag and subsequent elimination of the quencher from the molecular probe; rather, it is a combined effect for overall labeling. To avoid confusion arising from the similar emissive region for rhodamine isomers, they were treated separately in the mixtures with the other probes. This qualitative study of

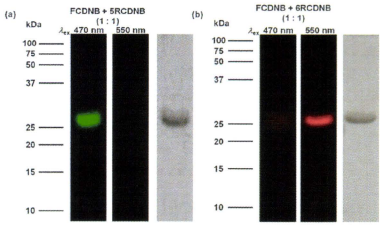

Fig. 4 Fluorescence (left) and CBB-stained (right) gel images of BL-tag incubated with (a) equimolar mixture of **5RCDNB** and **FCDNB** and (b) equimolar mixture of **6RCDNB** and **FCDNB**.

competitive protein labeling generates a preferential order among the fluorophores. From the mixture of the 5-rhodamine isomer and fluorescein derivatives, it was found that labeling was due to the fluorescein fluorophore (Fig. 4a). On the other hand, labeling was observed by the rhodamine fluorophore from the mixture of the 6-rhodamine isomer and fluorescein derivatives (Fig. 4b). These results conclude that the order of labeling probe is **6RCDNB** > **FCDNB** > **5RCDNB**. When the coumarin derivative was used in any binary mixture, the labeled protein showed the emission of coumarin irrespective of labeling by the other probes, except in the case of the 5-rhodamine isomer (Fig. S9 and S10, ESI†). In the case of a mixture of the coumarin derivative and the 5-rhodamine isomer, only coumarin fluorescence was observed without any rhodamine labeling. However, in the other cases, rhodamine and fluorescein fluorescence were observed from **6RCDNB** and **FCDNB**, respectively, along with the coumarin fluorescence when they were treated together with 1 : 1 molar ratio with **CCDNB**. The position of the coumarin derivative in the ordering of the probes could not be fixed from these qualitative SDS-PAGE studies. This result only supported the following labeling order: as **CCDNB** > **5RCDNB**. In the presence of an equimolar ternary mixture of **CCDNB**, **5RCDNB**, and **FCDNB**, the labeling due to coumarin and fluorescein was observed, without any fluorescence from rhodamine isomers. On the other hand, coumarin and rhodamine labeling were observed when a mixture of **CCDNB**, **6RCDNB**, and **FCDNB** was used (Fig. S11, ESI†).

Quantitative ordering of labeling efficiencies of the probes

All the qualitative results were further supported by the time-dependent fluorescence intensity measurement of the mixtures in the presence of the BL-tag. This quantitative measurement provided the order of labeling between all the probes from their mixtures. The fluorescence enhancement was monitored only at 450 nm (λ_{ex} = 407 nm) due to coumarin from its mixture with the other probes in the presence of the BL-tag (Fig. S12, ESI†). The enhancement rate supported the order of labeling obtained from SDS-PAGE studies for the rest of the probes. To find out the exact order of labeling efficiencies among **CCDNB**, **6RCDNB**, and **FCDNB**, fluorescence enhancement at 520 nm (λ_{ex} = 497 nm) and 575 nm (λ_{ex} = 558 nm) was monitored for the emission of fluorescein and 6-rhodamine, respectively, from the mixture of the probes. The fluorescence enhancement at 520 nm (Fig. 5a) suggests that the binding efficiency of **6RCDNB** is more compared to that of **CCDNB**. This is attributed to the lower fluorescence enhancement of fluorescein in the presence of the 6-rhodamine isomer compared to the case of fluorescein in the presence of the coumarin probe. A similar type of experiments used for the monitoring the fluorescent enhancement due to 6-rhodamine (Fig. 5b) was used to determine the binding efficiency order of the coumarin and fluorescein probes. The quantitative result generated the order **6RCDNB** > **CCDNB** > **FCDNB**. A combination of quantitative and qualitative results brought forth the overall binding efficiencies of the probe toward the BL-tag technique. The final order was found to be **6RCDNB** > **CCDNB** > **FCDNB** > **5RCDNB**. This ordering is the overall effect of disaggregation followed by the elimination step in BL-tag technology, and both of them are dependent upon the aggregation interactions between fluorophores and DNB quenchers.

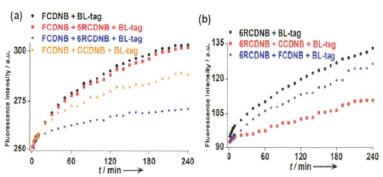

Fig. 5 (a) Time-dependent emission enhancement spectra (λ_{ex} = 497 nm and λ_{em} = 520 nm) of **FCDNB** (conc. of **FCDNB**: 1.0 μM) in presence of BL-tag with equimolar amounts of other probes in 100 mM HEPES buffer (pH 7.4) containing 0.1% DMSO at 25 °C. (b) Time-dependent emission enhancement spectra (λ_{ex} = 558 nm and λ_{em} = 575 nm) of **6RCDNB** (conc. of **6RCDNB**: 1.0 μM) in presence of BL-tag with equimolar amount of fluorescein and coumarin probes in 100 mM HEPES buffer (pH 7.4) containing 0.1% DMSO at 25 °C.

Protein labeling in living cells

In our present study, we used confocal microscopy for site-specific cell membrane labeling studies with the BL-tag fused with the N-terminus of the EGFR protein using fluorescein and coumarin fluorophore-based probes. We have chosen the probes according to their well-separated excitation wavelengths. HEK293T cells expressed with the BL-EGFR fusion protein were used for site-specific labeling of **CCDNB** and **FCDNB** (Fig. 6). Fluorescence images of the HEK293T cells were taken after probe treatment. Specific labeling of the cell membranes expressing the BL-EGFR fusion protein was observed with **CCDNB** (Fig. 6a). In the case of **FCDNB** (Fig. 6e), the cell membrane labeling was observed to be similar to that obtained in our previous experiment with an inverted fluorescence microscope.[13] On the other hand, in HEK293T cells expressed with the EGFR protein without any BL-tag, neither the coumarin- nor the fluorescein-labeled cell was observed (Fig. 6c and g).

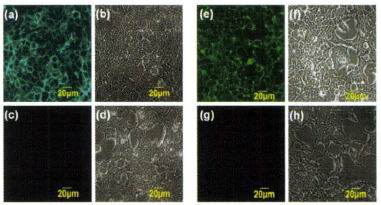

Fig. 6 Optical microscopic images of (a–d) **CCDNB** and (e–h) **FCDNB**-labeled HEK293T cells expressing (a,b,e,f) BL-EGFR and (c,d,g,h) EGFR. (a,c,e,g) Fluorescence microscopic images and (b,d,f,h) phase contrast microscopic images. For fluorescence microscopic images, the cells were excited by 405 nm and 473 nm laser lights for **CCDNB** and **FCDNB**, respectively.

Conclusions

In conclusion, we have developed a protein labeling method with comparative wide varieties of fluorophores involving a specific order for an aggregation and elimination-based BL-tag method. This technique is now established to be applicable without any restriction in the choice of the fluorophore, and more precisely, this technique has control over the reaction kinetics through the involved aggregation method. Based on appropriate demand of color for cell imaging, modification of the probe design is possible to get success in labeling of more than one targeted protein of interest. The color palette of this technique would help to combine this method with other methods known in the literature to tag different proteins in living cell simultaneously. Modification of the quencher part with more efficient quenched probes will help to obtain maximum fluorogenicity from this technique. We are now developing a method to reduce the incubation period in live cell imaging studies.

Experimental section

See supporting information for full experimental details and the labeling scheme of protons for assigning ^{1}H NMR of all the probes (Fig. S2 and S3) and other supporting materials, ESI.†

Synthesis of **CCDNB**. Compound **8** (Fig. S1, ESI†) (24 mg, 0.3 mmol) and 7-hydroxycoumarin-3-carboxylic acid *N*-succinimidyl ester (9 mg, 0.3 mmol) were dissolved in 0.5 mL of *N*,*N*-dimethylformamide. To this solution, TEA (3 mg, 0.3 mmol) was added at 0 °C (Scheme S1, ESI†). The reaction was continued for 6 h. The desired product **CCDNB** was isolated using preparative HPLC (10 mg, y. 34%). ^{1}H NMR (DMSO-d_6, 400 MHz) δ 1.72 (m, 2H, 2 × a), 1.88 (m, 2H, 2 × b), 3.39–3.57 (m, 22H, 1 × c, 1 × d, 2 × e, 2 × f, 4 × g, 8 × h, 2 × i, 2 × j), 4.08 (br, 1H, k), 5.07 (s, 1H, l), 5.18 (d, 1H, m), 5.48 (m, 1H, n), 6.81 (d, 1H, o), 6.88 (dd, 1H, p), 7.19 (d, 1H, q), 7.39 (d, 2H, 2 × r), 7.74 (d, 2H, 2 × s), 7.81 (d, 1H, t), 8.23 (dd, 1H, u), 8.41 (m, 1H, v), 8.77 (s, 1H, w), 8.83 (d, 1H, x), 8.96 (br, 1H, ya), 8.96 (m, 1H, yb), 11.09 (s, 1H, z); ^{13}C NMR (DMSO-d_6 100 MHz) δ 28.4 (a, b), 35.4 (e), 36.8 (i), 37.2 (f), 41.1 (j), 68.5 (m), 68.6 (n), 69.8 (c), 69.9 (g), 70.0 (h), 111.2, 115.3, 119.7, 122.2, 123.8, 125.5, 127.9, 129.7, 130.2, 132.0, 134.9, 139.5, 148.3, 148.5, 155.9, 156.6 (Ar), 163.7, 167.9, 168.1, 168.7, 169.4 (C=O); HRMS ($C_{43}H_{46}N_7O_{16}S_2$, FAB+); Found 980.2464; Calc., 980.2437.

Synthesis of **5RCDNB** and **6RCDNB**. Compound **8** (24 mg, 0.3 mmol) and 5(6)-carboxytetramethylrhodamine, succinimidyl ester (5(6)-TAMRA, SE) (16 mg, 0.3 mmol) were dissolved in 0.5 mL of *N*,*N*-dimethylformamide. To this solution, TEA (3 mg, 0.3 mmol) was added at 0 °C (Scheme S2, ESI†). The reaction was continued for 6 h. The desired products **5RCDNB** and **6RCDNB** were isolated using preparative HPLC.

5RCDNB (6.5 mg, y. 18%); ^{1}H NMR (DMSO-d_6, 400 MHz) δ 1.72 (t, 2H, 2 × a), 1.87 (t, 2H, 2 × b), 2.96 (s, 12H, c), 3.40–3.54 (m, 18H, 2 × d, 2 × e, 6 × f), 3.81–4.1 (m, 3H, 2 × j + h, i), 5.10 (s, 1H, w), 5.18 (d, 1H, l), 6.51–6.58 (br, 6H, m), 7.21 (d, 1H, n), 7.32 (d, 1H, p), 7.37 (d, 2H, 2 × o), 7.74 (d, 2H, 2 × q), 8.22 (d, 1H, r), 8.42 (d, 1H, t), 8.48 (s, 1H, s), 8.86 (s, 1H, u), 8.99–9.15 (br, 3H, 3 × v); ^{13}C NMR (DMSO-d_6 100 MHz) δ 28.3 (a, i), 29.4 (b), 31.2 (g), 36.7 (e), 41.2, 42.6, 44.4 (c, d, j), 60.3 (k, l), 68.3, 73.6 (f), 98.1 (m), 115.2 (n), 119.5, 119.8, 120.5, 121.9, 122.6, 123.6, 125.9, 126.6, 127.3, 127.7, 128.6, 129.6, 130.0, 131.1, 134.6, 148.4 (Ar), 164.6, 165.1, 165.5, 168.4, 169.4, 169.8 (C=O); HRMS ($C_{58}H_{62}N_9O_{16}S_2$, FAB+); Found 1204.3783; Calc., 1204.3750.

6RCDNB (5 mg, y. 14%); ^{1}H NMR (DMSO-d_6, 400 MHz) δ 1.71 (t, 2H, 2 × a), 1.86 (t, 2H, 2 × b), 2.95 (s, 12H, c), 3.40–3.54 (m, 18H, 2 × d, 2 × e, 6 × f), 3.81–3.89 (m, 3H, 2 × j + h), 4.06 (d, 1H, i), 5.00 (br, 1H, w), 5.12 (d, 1H, l), 6.51 (br, 6H, m), 7.21 (d, 1H, n), 7.37 (d, 2H, 2 × o), 7.66 (s, 1H, p), 7.74 (d, 2H, 2 × q), 8.08 (d, 1H, r), 8.15 (d, 1H, s), 8.25 (d, 1H, t), 8.85 (d, 1H, u), 8.99 (br, 3H, 3 × v); ^{13}C NMR (DMSO-d_6 100 MHz) δ 28.2 (a, i), 29.3 (b, g), 36.6 (e), 41.0 (c, d, j), 60.3 (k, l), 68.2, 69.6, 69.7, 69.8 (f), 97.9 (m), 115.1 (n), 121.3, 123.6, 127.4, 127.8, 128.5, 129.6, 130.0, 131.8, 134.6, 135.6, 139.6, 140.8, 144.3, 148.3, 152.5, 153.6 (Ar), 162.1, 163.6, 165.0, 165.5, 168.1, 169.5 (C=O); HRMS ($C_{58}H_{62}N_9O_{16}S_2$, FAB+); Found 1204.3729; Calc., 1204.3750.

Acknowledgements

This research is supported by the Japan Society for the Promotion of Science (JSPS) through its "Funding Program for World-Leading Innovative R&D on Science and Technology (FIRST Program)." This work was supported in part by the CREST funding program from the Japan Science and Technology Agency (JST); a Grant-in-Aid for Scientific Research from the Ministry of Education, Culture, Sports, Science and Technology (MEXT) of Japan; and a Grant-in-Aid from the Ministry of Health, Labour and Welfare (MHLW) of Japan. KKS and SW acknowledge support from a Global COE Fellowship of Osaka University. SW acknowledges a JSPS Research Fellowship.

Notes and references

1 (*a*) Z. Zhou, A. Koglin, Y. Wang, A. P. McMahon and C. T. Walsh, *J. Am. Chem. Soc.*, 2008, **130**, 9925–9930; (*b*) S. S. Gallagher, J. E. Sable, M. P. Sheetz and V. W. Cornish, *ACS Chem. Biol.*, 2009, **4**, 547–556; (*c*) R. McRae, P. Bagchi, S. Sumalekshmy and C. J. Fahrni, *Chem. Rev.*, 2009, **109**,